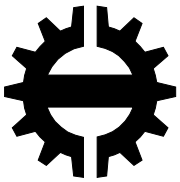

TAMPERE UNIVERSITY OF TECHNOLOGY
Department of Communications Engineering

Md. Sarwar Morshed

Synchronization Performance in DVB-T2 System

Master of Science Thesis

Subject approved by the Council of the Faculty of Computing and Electrical Engineering on 04.03.2009

Supervisors: Lic. Tech. Jukka Rinne
Dr. Ali Hazmi

Abstract

Tampere University of Technology

Master's Degree Programme in Information Technology

Morshed, Md. Sarwar: Synchronization Performance in DVB-T2 system

Master of Science Thesis, 75 pages

September 2009

Major: Communications Engineering

Supervisors: Lic. Tech. Jukka Rinne, Dr. Ali Hazmi

Keywords: DVB-T2, OFDM, Synchronization

The Digital Video Broadcasting (DVB) project has developed digital broadcasting system specifications which have been adapted worldwide. The family of DVB standards includes DVB-S for satellite, DVB-C for cable and DVB-T for terrestrial system. This DVB-T system has proven its capability and thus accepted as the standard for terrestrial system in most countries. DVB-T2 is the enhancement of DVB-T that will overcome the shortcomings of the previous standard and provide additional features.

This thesis concentrates on synchronization performance in DVB-T2 systems. Synchronization is the most important task that the receiver has to perform in the beginning of its reception of the signal. DVB-T2 uses Orthogonal Frequency Division Multiplexing (OFDM) modulation method and has a special symbol, named P1 symbol, for performing initial synchronization tasks. This symbol is also used for detecting DVB-T2 signal, meaning that, if the receiver can detect the P1 symbol, then it can conclude that the channel contains DVB-T2 signal. Moreover, P1 symbol also transmits basic transmission parameters that the receiver needs in the first place in order to proceed for further processing.

In this work, the DVB-T2 system model has been implemented including the P1 symbol and the performance of synchronization by P1 symbol has been analyzed extensively by simulations in different channel conditions. P1 symbol deals with the synchronization issues before performing Fast Fourier Transform (FFT). Therefore, P1 symbol based methods can achieve coarse timing synchronization and fine frequency synchronization. Also the detecting and decoding probabilities based on P1 symbol in different channels are presented in this thesis.

Preface

This Master of Science Thesis has been written for the Master's Degree Programme in Information Technology under the Faculty of Computing and Electrical Engineering. The work for this thesis has been performed under the DVB project group at the Department of Communications Engineering (DCE) of Tampere University of Technology (TUT), Tampere, Finland. This work was done under the European project named EUREKA/CELTIC B21C, funded by Tekes, The Finnish Funding Agency for Technology and Innovation.

I would like to express my sincere and deep gratitude to the Head of the DCE, Professor Markku Renfors for giving me the opportunity to be a part of the DVB research group and thus offering me to enjoy the wonderful research and work environment at DCE.

I wish to express my heartfelt appreciation to my supervisors Lic. Tech. Jukka Rinne and Dr. Ali Hazmi for their tremendous support, valuable guidance and infinite tolerance during my work in the research group. It was a great pleasure to receive help from my supervisors always with warm welcome whenever I needed.

I also want to thank my Bangladeshi friends in Tampere for their enjoyable company during the days of my M.Sc. studies. Special thanks to Mohammad Zahidul Hasan Bhuiyan, who inspired me to come to Finland back in February 2006.

I am indebted to my parents, Md. Abdul Hamid and Sharifa Akhter, little brother Md. Sarwar Muyeed, and grandmother Shaharjan Begum for their endless love and encouragement. I would not be able to come this far if my father was not successful in convincing me to take this path. Whenever I felt down, my family was always with me with their affection.

Finally this endeavor is dedicated to my beautiful wife, Rubaiya Mannan, for her love, emotional support, and for making my days shine.

In Tampere, Finland, September 12, 2009.

Md. Sarwar Morshed

Orivedenkatu 8 D 79
33720 Tampere, Finland
morshed04@gmail.com

Table of Contents

List of Abbreviations

ACE	Active Constellation Extension
AWGN	Additive White Gaussian Noise
BCH	Bose-Chaudhuri-Hocquengham
BER	Bit Error Rate
BICM	Bit Interleaved Coding and Modulation
CDS	Carrier Distribution Sequence
CRC-8	Cyclic Redundancy Check-8
CW	Continuous Wave
DAB	Digital Audio Broadcasting
DBPSK	Differential Binary Phase Shift Keying
DFT	Discrete Fourier Transform
DVB-T	Digital Video Broadcasting – Terrestrial
DVB-T2	The Digital Video Broadcasting – Terrestrial version 2
ETSI	European Telecommunications Standards Institute
FEC	Forward Error Correction
FEF	Future Extension Frame
FFT	Fast Fourier Transform
GI	Guard Inteval
ICI	Inter-Carrier Interference
IDFT	Inverse Discrete Fourier Transform
IFFT	Inverse Fast Fourier Transform
ISI	Inter-Symbol Interference
LDPC	Low Density Parity Check
LOS	Line Of Sight
MCM	Multi Carrier Modulation

MFN	Multi Frequency Network
MISO	Multiple Input Single Output
MSE	Mean Squared Error
NLOS	Non-Line Of Sight
OFDM	Orthogonal Frequency Division Multiplexing
QAM	Quadrature Amplitude Modulation
QPSK	Quadrature Amplitude Shift Keying
PAPR	Peak to Average Power Ratio
PLP	Physical Layer Pipes
PRBS	Pseudo-Random Binary Sequence
RF	Radio Frequency
RS	Reed Solomon
SFN	Single Frequency Network
SISO	Single Input Single Output
SNR	Signal to Noise Ratio
SSI	Self-Symbol Interference
TPS	Transmission Parameter Signalling
TR	Tone Reservation
TU6	Typical Urban-6
VLSI	Very Large Scale Integration
WLAN	Wireless Local Area Network
WiMAX	Worldwide interoperability for Microwave Access

List of Important Symbols

f_d	Doppler shift
f_k	Carrier frequency at *k*th symbol
f_0	First carrier frequency
f_{SH}	Frequency shift
g_k	Time limited complex exponential
K	Ricean factor
k	Subcarrier number
k_{P1}	Indices of active carriers
MOD_SCR_i	Modulation values for active carriers
N	Total number of subcarrier or FFT size
n	Subcarrier number
$P_1(t)$	Time domain baseband waveform
$P(\tau_e)$	Average received power
T	Elementary time period
T_A	Part A of P1 symbol
T_B	Part B of P1 symbol
T_C	Part C of P1 symbol
T_m	Multipath delay spread
T_s	Total symbol duration
T_u	Useful symbol duration
$X_{n,k}$	Complex transmitted data symbol
$x(t)$	Transmitted signal
$Y_{n,k}$	Complex received decision variable
$y(t)$	Received signal
Δ_g	Guard interval

$(\Delta f)_c$	Coherence bandwidth
$(\Delta f)_{ds}$	Doppler shift
$(\Delta t)_c$	Coherence time
θ_i	Phase shift from scattering of the *i*th path
ρ_i	Attenuation of the *i*th path
ρ_0	The line of sight ray
τ_d	Delay spread
τ_e	Excess time delay
τ_i	Relative delay of the *i*th path
$\varphi_{n,k}(t)$	Elementary basis function

1. Introduction

Digital transmission has earned tremendous popularity in the terrestrial TV-broadcasting area in the last decade. The specification phase of digital television started in Europe in 1993 and was lead by DVB (Digital Video Broadcasting) project [1]. It is an industry-led consortium of broadcasters, manufacturers, network operators, software developers, and regulatory bodies. At the beginning, DVB started its work to establish standards to enable the delivery of digital TV to the consumer. Therefore three different standards were proposed by DVB during this starting phase for different system specifications: DVB-S for satellite system, DVB-C for cable system, DVB-T for terrestrial system [2]. There is another DVB standard, named DVB-H for handheld [3], which is basically an extension to the DVB-T standard and is meant for handheld mobile terminals.

The Digital Video Broadcasting – Terrestrial (DVB-T) specification was first published in 1997 [2]. DVB-T is designed to allow optimum use of available frequency spectrum. Moreover, the structure of broadcast data is flexible enough to accommodate numerous services. It is also a flexible system that supports fixed, portable, and mobile reception. The analog television broadcasting is currently replaced by the digital terrestrial television in many countries.

After the success of the first standard in digital broadcasting area, suggestions were coming to improve the quality of service provided by DVB-T. Originally DVB-T standard was developed for stationary reception with directional roof-top antenna or portable reception with non-directional antenna. However, new services are emerging for portable devices that may require reception inside buildings or running vehicles. Thus DVB-T was facing some challenges. At this point, the need of a new standard

came into scenario that will have all the facilities of the previous system, but will enhance the performance where the previous one was not able to provide. This led to the standardization of Digital Video Broadcasting-Terrestrial version 2 (DVB-T2) [4].

Broadcasting video information in digital format has some advantages compared to conventional analog transmission which includes better picture quality, reduced channel bandwidth, interactivity with viewer, providing mobile reception. However, digital system has problems of different types. For instance, synchronization is an important issue in digital system. If synchronization is not achieved, then further decisions taken in the receiver might be wrong.

This thesis focuses on the synchronization issues of the digital system DVB-T2. It also focuses on the special symbol used in DVB-T2 for detecting the presence of the T2 signal in the channel. This special symbol, called P1 symbol, also carries out some transmission parameters that the receiver needs to decode in the very beginning. The work of this thesis was carried out while participating in the European project, named EUREKA/CELTIC B21C (Broadcast for the 21st Century) contributing to the DVB-T2 standard implementation verification.

The thesis is organized into seven chapters. After introducing the subject matters in the first Chapter in introduction, the principle of Orthogonal Frequency Division Multiplexing (OFDM) modulation method of DVB-T2 is discussed in Chapter 2. Then, the DVB-T2 system is elaborated in Chapter 3 that provides sufficient background knowledge about this system. This chapter also presents the comparison between DVB-T2 system and its previous DVB-T system. The channel models are very important for assessing technology for wireless systems. Hence Chapter 4 discusses about signal propagation and channel parameters along with wireless channel models that have been used in performance evaluation.

The theoretical synchronization schemes for OFDM and the important synchronization issues in DVB-T2 that can be achieved by P1 symbol are discussed in Chapter 5. The evolution stages of P1 symbol structure and corresponding receiver processing chains from simple guard interval structure to a complex one is also presented in this chapter. Chapter 6 presents the simulation model and related simulation results for analyzing the performance of P1 symbol. Finally, Chapter 7 concludes and summarizes the main result of the thesis.

2. Principles of OFDM

This chapter describes the basic principles of Orthogonal Frequency Division Multiplexing (OFDM) that is used in many modern high-speed digital communication systems. Various applications like Digital Video Broadcasting (DVB-T), Digital Audio Broadcasting (DAB), Wireless LAN (WLAN), and Worldwide interoperability for Microwave Access (WiMAX) are using OFDM to transfer data because of its advantages over other single and multi-carrier transmission systems.

2.1. OFDM basics

OFDM is a special form of Multi Carrier Modulation (MCM). In this technique, the high-rate serial data-stream is converted to low-rate parallel data-streams in the transmitter side. Also the available channel bandwidth is divided into a number of sub-channels where each sub-channel is nearly ideal and orthogonal to others. Then the low-rate data-streams are modulated to these sub-channels on different frequencies simultaneously [5]. As a result of that, the transmission system has many parallel data elements at any instant of time. Therefore, instead of taking all the available bandwidth like a conventional serial data transmission system, the spectrum of an individual data element in OFDM system will occupy only a small portion of the available bandwidth [6].

OFDM can tolerate frequency selective fading. The narrow-band frequency selective fades can destroy only the data-streams of some sub-channels in OFDM, which is better than single carrier systems where one single fade can destroy many sequential data-streams. Effective error correction scheme can recover the destroyed data partially in OFDM, rather than completely being destroyed like single carrier

systems. [6] Moreover, Inter-Symbol Interference (ISI) can be completely eliminated by including guard interval in every OFDM symbol. Furthermore, Inter-Carrier Interference (ICI) can be eliminated by cyclically extending the OFDM symbol [7].

The OFDM technique is bandwidth efficient compared to conventional non-overlapping multicarrier systems. As shown in Figure 2.1, adjacent sub-channels are allowed to overlap in OFDM provided that they are orthogonal to each other. It is better than conventional non-overlapping multicarrier systems where frequency gaps are inserted between channels to avoid adjacent carrier interference in [6]. Also the long symbol period of OFDM made it robust against impulse noise and fast channel fades [5]. Moreover, one tap equalizer is enough in the receiver to receive the signals in each sub-channel [8]. All in all, OFDM allows implementing single frequency networks, which is beneficial for broadcasting applications.

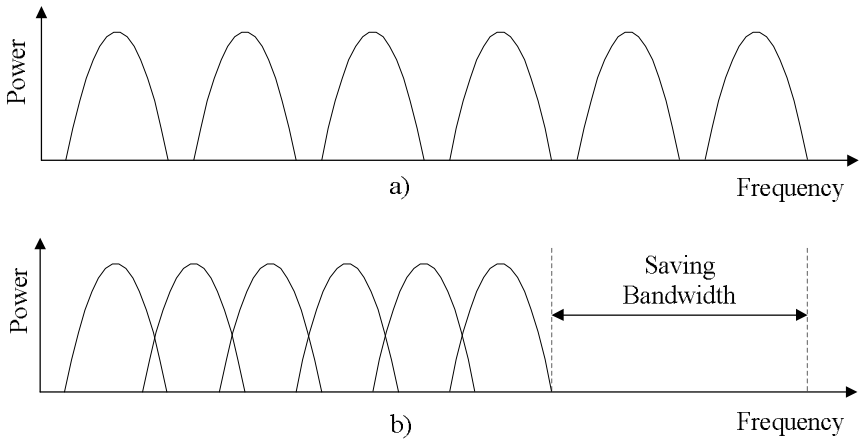

Figure 2.1. *a)Conventional non-overlapping multicarrier system b)OFDM system [6].*

2.2. OFDM signal

In OFDM, the subcarriers are modulated in frequency domain, then they are converted to time domain and after that, guard interval is added before transmission. Therefore it enables a different approach to channel equalization. The OFDM signal and guard interval are explained in the following sections.

2.2.1 Mathematical definition

Let us consider that the useful symbol duration is represented by T_u. Then the spacing of the subcarriers is $1/T_u$ and the subcarrier frequencies can be expressed as

$$f_k = f_0 + \frac{k}{T_u}, \qquad k \in [0, N-1] \tag{2.1}$$

where f_0 is the first carrier frequency and N is the total number subcarriers. The elementary basis function can be given as [9]

$$\phi_{n,k}(t) = g_k\ (t - nT_u) \tag{2.2}$$

Where g_k is the time limited complex exponential represented as:

$$g_k = \begin{cases} e^{i2\pi f_k t} & , 0 \le t < T_u \\ 0 & , otherwise \end{cases} \tag{2.3}$$

When the orthogonality theorem is applied to the elementary signals given in previous equations, it follows that:

$$\int_{-\infty}^{\infty} \phi_{n,k_1}(t)\ \phi^*_{n,k_2}(t)\, dt = \begin{cases} T_u & , k_1 = k_2 \\ 0 & , k_1 \neq k_2 \end{cases} \tag{2.4}$$

Therefore the orthogonality condition is satisfied. The modulation of complex data symbols $X_{n,k}$ is done for each symbol at corresponding carrier frequency f_k. Then each modulated signals are summed and transmitted through the channel. The transmitted OFDM baseband signal in time domain can be mathematically expressed as [9]:

$$x(t) = \sum_{n=-\infty}^{\infty} \sum_{k=0}^{N-1} X_{n,k}\ \phi_{n,k}(t) \tag{2.5}$$

where $X_{n,k}$ is the complex data symbol of the n^{th} carrier at the k^{th} OFDM symbol and N is the number of carriers. The spectrum of each modulated subcarrier will be a sinc-function with this type of modulation. In the receiver, the received signal $y(t)$ is demodulated according to the Fourier integrals and mathematically expressed as:

$$Y_{n,k} = \frac{1}{T_u} \int_{-\infty}^{\infty} x(t)\ \phi^*_{n,k}(t)\, dt \tag{2.6}$$

where $Y_{n,k}$ is the decision variable of the n^{th} carrier at the k^{th} symbol. An example spectra of and OFDM sub-channel and OFDM signal are presented in Figure 2.2.

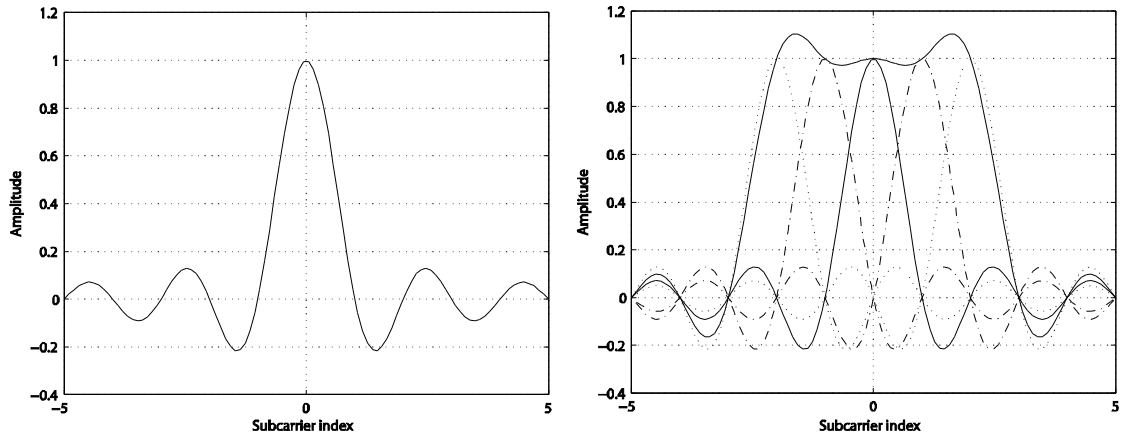

(a) (b)

Figure 2.2. *Spectra of a) an OFDM sub-channel, and b) an OFDM Signal.*

2.2.2 Guard interval

In practical OFDM systems, the orthogonality of sub-channels cannot be maintained and individual sub-channels cannot be completely separated by the Fast Fourier Transform (FFT) in a receiver because ISI and ICI are introduced by the transmission channel. In presence of multipath propagation in the transmission channel, a receiver will receive many copies of the originally transmitted signal. As a result, there will be ISI between two or more consecutive OFDM symbols because a continuous stream of OFDM symbols were transmitted from the transmitter. This ISI can be eliminated by adding a guard interval (Δ_g) to each OFDM symbol [6].

To remove ISI properly, the duration of the guard interval must be longer than the channel delay spread, represented by τ_d. Delay spread is the time difference between the first and the last multipath component. After using the guard interval, the total symbol duration (T_s) of an OFDM symbol leaving the transmitter antenna will be the summation of useful symbol duration (T_u) and guard interval duration (Δ_g) as below:

$$T_s = T_u + \Delta_g \qquad (2.7)$$

However, guard interval does not remove Self-Symbol interference (SSI). SSI is the interference between the samples of the same OFDM symbol. But SSI can be easily equalized in the receiver. If this guard interval is set to all zeros, then still there might be a problem of ICI, i.e., the problem of the sub-channels not being orthogonal to each other. To remove ICI, the concept of cyclic prefix is used. It means that each

of the OFDM symbol is cyclically extended [7] because the guard interval is copied from the end of an OFDM symbol and placed as a prefix on that same symbol.

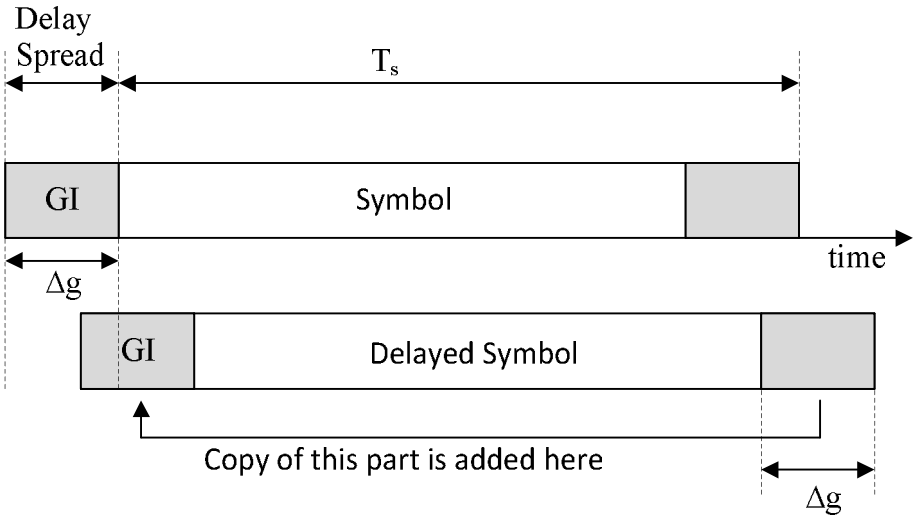

Figure 2.3. *Cyclic prefix in a multipath channel.*

An OFDM symbol and its delayed version are presented in Figure 2.3 to show the effect of cyclically extended guard interval. As long as the delayed version is within the guard interval, ISI will not be introduced as the useful part of the OFDM symbol is preserved. This guard interval can be used for symbol synchronization and delay spread estimation in the receiver and later on will be removed before demodulation.

2.3. OFDM Implementation

An OFDM signal can be implemented by using Discrete Fourier Transform (DFT) [10] with low complexity. To produce modulated and sampled OFDM signal, the transmitted signal of Equation (2.5) can be implemented by *N*-point Inverse Discrete Fourier Transform (IDFT) as follows

$$x(n) = IDFT\ (X(k)) = \sum_{k=0}^{N-1} X(k)\, e^{\frac{i2\pi kn}{N}}\ ,\ n = 0....N-1 \qquad (2.8)$$

Correspondingly in the receiver, the demodulation can be performed by DFT as given below:

$$X(k) = DFT\ (x(n)) = \frac{1}{N}\sum_{n=0}^{N-1} x(n)\, e^{-\frac{i2\pi kn}{N}} \quad , \ k = 0....N-1 \qquad (2.9)$$

The discrete Fourier transforms can be calculated by using FFT when fast computation is needed. The reason is FFT has a computational complexity of $O(Nlog_2N)$ whereas DFT has a complexity of $O(N^2)$. Moreover, recent progress of Very Large Scale Integration (VLSI) and digital signal processing technologies provide good opportunities to implement OFDM in hardware by simple FFT and IFFT.

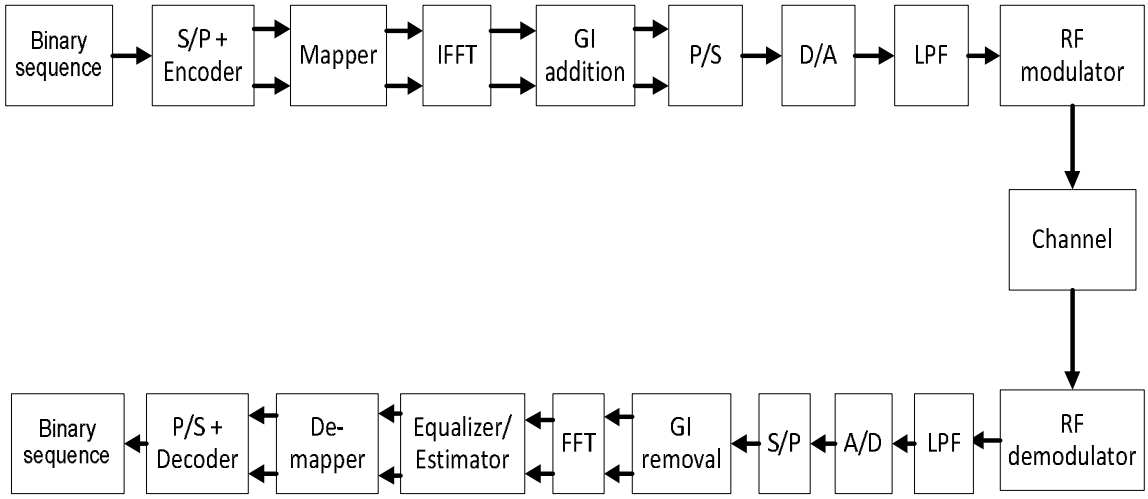

Figure 2.4. *A block diagram of OFDM transmitter and receiver.*

A basic system level block diagram of OFDM transmitter and receiver using IFFT/FFT is presented in Figure 2.4. In the transmitter, at first the serial binary sequence coming from data source is converted to parallel and grouped into a number of bits. Then mapper maps these groups of bits according to the selected modulation scheme in order to produce complex symbol sequence. These symbols are then modulated in the baseband by the IFFT operation and after that, guard interval is added to each symbol. Afterwards, the parallel data stream is converted to serial data stream for transmission by parallel-to-serial (P/S) converter. This discrete signal is then transformed into analog domain by the digital-to-analog (D/A) converter and a low pass filter. And at last, the baseband signal is shifted to passband by the Radio Frequency (RF) modulator and the signal is now ready for transmission.

In the receiver, the reverse operations of the transmitter take place in a reverse order to reproduce the transmitted binary sequence. At first, the RF demodulator shifts the received signal from passband to baseband and after that, the analog signal is transformed to digital signal by the analog-to-digital (D/A) converter. Then the serial digital symbol stream is converted to parallel symbol streams by serial-to-parallel (S/P) converter. Afterwards, the guard interval is removed and the parallel symbols streams are demodulated by the FFT operation.

The received signal suffers from some unwanted degradation effects by the channel. In order to minimize those unwanted effects, an equalizer or estimator is placed in the receiver after the FFT operation and before performing the de-mapping operation. After equalizing and estimating the channel effects, de-mapping operation is performed and then the parallel stream is again converted to serial stream. The decoder used in the receiver is a soft decoder that takes the reliability of each bit into account while taking the decisions. As a result, the transmitted binary sequence is reproduced in the receiver.

2.4. Single frequency networks

OFDM gives the flexibility to implement Single Frequency Networks (SFN) where a number of transmitters synchronously broadcast the same program within the service area using the same frequency [11]. This is possible because OFDM system overcomes the problem of multipath interference. SFN has clear advantages over analog Multi Frequency Networks (MFN) because the latter one uses different frequencies for different transmitters. Therefore SFN has high spectrum efficiency, low installation cost requirement, more fault-resistance, and coverage improvement due to diversity gains [12]. Moreover, the power requirement of SFN for transmitting signal in a certain area is much lower than MFN as few low power transmitters can be used rather than using one high power transmitter.

In SFN, receivers will be able to receive ISI free signals on the same frequency from different transmitters as long as all the signal components reach the receiver within the cyclic prefix duration [11]. Moreover, it will give a constructive contribution to the useful signal energy. Furthermore, delayed signal components from more distant transmitters relative to the signal components from closer transmitters are treated as artificial multipath. Therefore the SFN system will not be hampered by these artificial multipath components.

2.5. Drawbacks

Though OFDM has several notable advantages but it has some drawbacks as well. For example, OFDM is more sensitive to carrier frequency offset. In ideal case, frequency of local oscillator in both transmitter and receiver will be same to ensure synchronization between them. However, frequency offset is originated when there is a mismatch between frequencies of local oscillator in the transmitter and in the receiver or when there is a Doppler shift caused by the relative speed of the transmitter and receiver. Because of this frequency offset, phase will be shifted, the desired signal level will be decreased and ICI will be introduced. Therefore, the Signal to Noise Ratio (SNR) will be decreased and as a result, the overall performance of the OFDM system will be degraded [13] [14].

OFDM also suffers in the presence of phase noise, which is originated due to oscillator non-ideality of transmitter and receiver. Phase noise is referred to the phase difference between the phase of the carrier signal and the phase of the local oscillator. Phase noise may be responsible to introduce common phase error, i.e., the common rotation of all constellation points in the complex plane, and it may also destroy the orthogonality between subcarriers because of the leakage of the DFT [15]. Furthermore, phase noise also reduces the effective SNR at the receiver and accordingly the Bit Error Rate (BER) and data rate will be limited. Most importantly, it is difficult to track and eliminate phase noise in OFDM systems compared to single carrier systems [16].

Another major drawback of OFDM is its high Peak to Average Power Ratio (PAPR). It means that if the peak transmit power is reduced much, then the average power will be decreased in such a way that the range of MCM will be reduced. Moreover, if the power is reduced in order to make the power amplifier to operate in its linear region, then it results input back–off and inefficient use of the amplifier. All in all, the drawbacks of PAPR may destroy all the potential benefits of MCM as a whole [17].

3. Overview of the DVB-T2 system

Digital Video Broadcasting–Terrestrial version 2 (DVB-T2) is the second generation Digital Terrestrial Transmission (DTT) system standard [4]. It is developed on top of the DVB-T standard [2] in order to provide additional facilities and features. DVB-T2 uses latest modulation, coding and error correction techniques in order to enable highly efficient use of valuable terrestrial spectrum. This chapter gives an overview about the old DVB-T system, introduces the need for new DVB-T2 system, and then gives a brief overview of DVB-T2 system along with the differences between the old and the new system according to the standard [2] [4] in order to present the background information for the following chapters.

3.1. DVB-T System Overview

The finalized standard for DVB-T was published in 1997 by European Telecommunications Standards Institute (ETSI) [2] that essentially defined a way for transmitting MPEG-2 source coded data terrestrially. DVB-T uses OFDM with options for Quadrature Amplitude Shift Keying (QPSK), 16-Quadrature Amplitude Modulation (QAM) or 64-QAM modulation and supports 6, 7 or 8 MHz channel bandwidth with 2k or 8k number of carriers. It also has two levels of coding and interleaving in order to provide robust performance. The system level block diagram of DVB-T is given in Figure 3.1.

DVB-T standard includes MPEG-2 source coding, followed by MUX adaptation, outer channel coding, outer interleaver and inner channel coding. All these blocks may have multiple instances which are indicated by shadows in the block diagram (Figure 3.1). After the inner channel coding block, DVB-T has consecutive

blocks for inner interleaver, mapper, frame adaptation, frame builder, IFFT, guard interval insertion and digital-to-analog (D/A) converter. Meanwhile signalling information is supplied to the frame adaptation block by the pilot and Transmission Parameter Signalling (TPS) signal block.

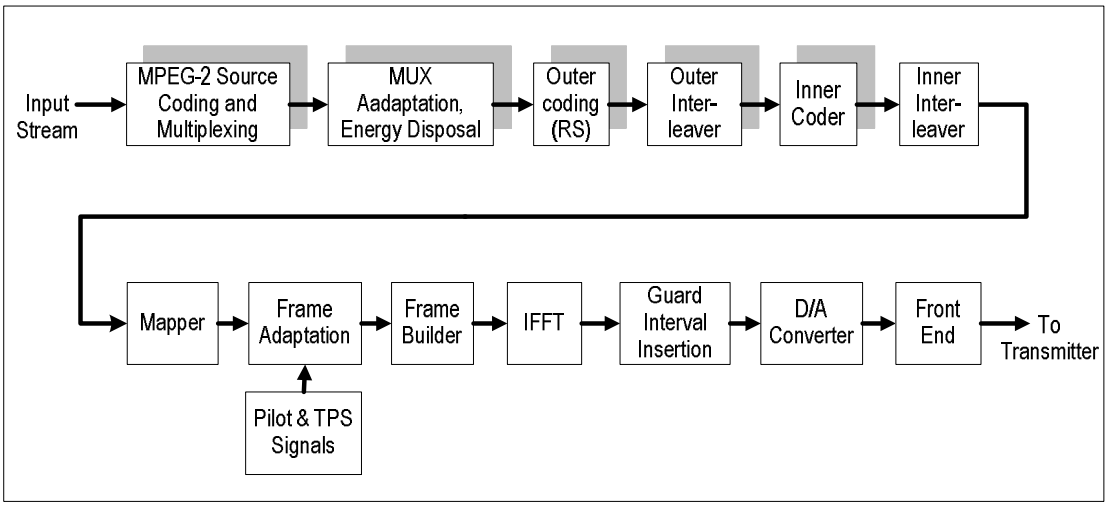

Figure 3.1. *DVB-T system block diagram [2].*

The MPEG-2 coded data to be transmitted is first multiplexed into fixed sized packets. The data of the input MPEG-2 multiplex is randomized for energy disposal by a Pseudo-Random Binary Sequence (PRBS) to ensure adequate binary transition. The packets are then passed to the outer channel coding and outer interleaver blocks. Outer coding is performed by Reed-Solomon (RS) coder that generates and appends the parity check bits at the end of the original packet. After that, outer interleaving is performed which is followed by punctured convolutional code based inner coding and inner interleaving. This inner interleaving consists of block-based bit-wise and symbol-wise interleaving. After that, the mapper maps the bits to constellation points based on the chosen modulation option.

At this point, frame adaptation module prepares an OFDM frame by organizing data, scattered pilots, continual pilots and Transmission Parameter Signalling (TPS). Each OFDM frame has 68 symbols and four OFDM frames comprise a super frame. Moreover, each OFDM symbol is constituted by either 2k or 8k carriers and is divided into cells, where each cell corresponds to one carrier modulated with either data or pilot or TPS during one symbol. The pilots are the cells within an OFDM symbol that has predefined values in order to perform frame

synchronization, frequency synchronization, time synchronization, channel estimation, transmission mode identification and phase noise reduction. On the other hand, TPS carriers are used to transmit signalling parameters for channel coding and modulation.

When frame builder block finishes creating a frame, then IFFT is performed to convert the signal from frequency domain to time domain. Afterwards guard interval is added in front of each frame which is a cyclic continuation of the useful part of the frame. Lastly the frames go through a digital-to-analog (D/A) converter and become ready for transmission and then they are supplied to the transmitter front-end in order to transmit.

3.2. DVB-T2 Requirements Overview

Although DVB-T standard was published in March 1997 and is now the most widely used DTT standard, but a new DTT standard seemed to be necessary to meet the need of the broadcasters of 21st century. This is the fact that motivated the researchers to develop a new updated DTT standard known as DVB-T2. It is the successor of DVB-T, thus it inherits many features of DVB-T and adds many additional features.

The new DVB-T2 standard must be developed in such a way that it should be compatible with the old DVB-T standard in order to reuse the existing transmitter infrastructures and receiver installations of the old standard. The preliminary target of DVB-T2 should be to increase the capacity as compared to DVB-T while providing services to fixed and portable devices. This new standard should also try to improve the performance in single frequency networks. It's another goal should be to include some technique to reduce the Peak to Average Power Ratio (PAPR) in order to reduce the cost of transmission. In addition, DVB-T2 should also provide flexibility of bandwidth and frequency along with the mechanism for providing service specific robustness. For example, roof-top reception and portable reception should be provided simultaneously within a single channel bandwidth. All in all, these are the potential requirements that DVB-T2 should try to fulfill [18].

3.3. DVB-T2 System Architecture

A generic block diagram of DVB-T2 system is presented in Figure 3.2. There may be multiple copies of the sub-modules depending on the number of Physical Layer Pipes (PLPs), which are represented by the shadows behind the sub-modules.

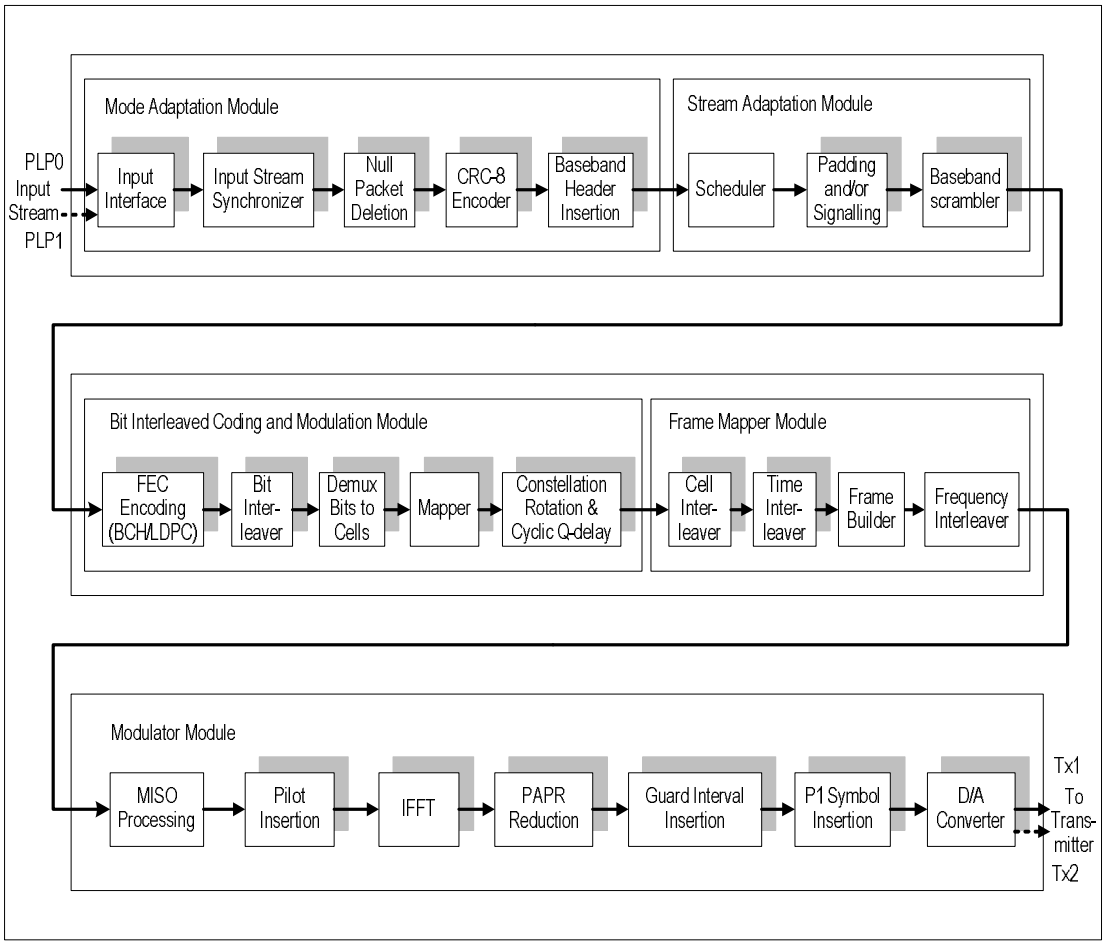

Figure 3.2. *DVB-T2 system block diagram [4].*

The input of the system may be one or more transport streams or generic streams whereas the output of the system may be one or more OFDM signals in order to transmit on RF channels. The system block diagram has several major modules, namely mode adaptation, stream adaptation, bit interleaved coding & modulation, frame mapper and the modulator module [4]. Every module has a number of sub-modules in order to carry out the module specific tasks.

3.4. DVB-T2 System Features

The principle system features of DVB-T2 system are presented briefly in the following subsections.

3.4.1 Mode adaptation

At the beginning of the DVB-T2 system, the input interface may have input preprocessor that takes transport streams or generic streams as inputs. Afterwards the service splitter inside the input preprocessor may split the services of transport streams into logical data streams, which are then carried by individual PLP. Later mode adaptation module individually works on the contents of each PLP by slicing the data stream into data fields and adds baseband header at the start of each field. The sub-modules of mode adaptation module are the input interface, three optional sub-modules: input stream synchronizer, null packet deletion and Cyclic Redundancy Check-8 (CRC-8) encoder, and baseband header insertion.

3.4.1.1 Input interface

Input interface works on each PLP individually and its main task is to convert the input electrical format to logical bit format. In doing this, it indicates the first received bit as the most significant bit.

3.4.1.2 Input stream synchronizer

The goal of input stream synchronizer is to provide constant bit rate and constant end-to-end transmission delay for every input format. It tries to minimize the effect of variable amount of transmission delay that the input data may have because of data processing by DVB-T2 modulator.

3.4.1.3 Null packet deletion

Null packets may be present in some transport stream input signals to adapt variable bit rate services into a constant bit rate transport stream. Therefore null packet deletion sub-module will identify and delete these null packets to avoid useless transmission overhead. Later these null packets can be added in their actual position in the receiver in order to maintain constant bit rate.

3.4.1.4 CRC-8 encoder

CRC-8 encoder sub-module uses a systematic 8-bit encoder in order to detect errors at user packet level and baseband header level. Afterwards the computed CRC-8 is added after the user packet.

3.4.1.5 Baseband header insertion

This sub-module chooses a 10 bytes baseband header format (Figure 3.3) depending on the normal or high efficiency mode and appends it in front of the baseband data field in order to clarify the format of the data.

3.4.2 Stream adaptation

Stream adaptation module takes a baseband header followed by a data field and makes a baseband frame. It comprises of three sub-modules: scheduler, inband signalling and baseband scrambler.

3.4.2.1 Scheduler

The scheduler sub-module counts the number of Forward Error Correction (FEC) frames for each PLP of the physical layer frame and forwards the counted value for insertion as inband signalling data. It also uses sub-slicing and sub-frame parameters in order to generate L1-signalling data.

3.4.2.2 Padding and/or signalling

When the baseband frame has insufficient data to fill it up or has the requirement to have an integer number of user packets, then padding is used to append zero bits after the data field to fill the frame. Moreover, padding field carries inband signalling information when the input mode is high efficiency mode (Figure 3.3).

3.4.2.3 Baseband scrambler

The main purpose of baseband scrambler is to ensure that the complete baseband frame is randomized. In addition, there must be synchronization between the randomization sequence and the baseband frame.

3.4.3 Bit interleaved coding and modulation

Bit Interleaved Coding and Modulation (BICM) module takes a baseband frame as input and produces an output for the next frame mapper module. To carry out this task, the BICM module performs FEC encoding, bit interleaving, de-multiplexing bits to cells, mapping cells to constellation points, and at last constellation rotation and cyclic Q-delay.

3.4.3.1 FEC encoding (BCH/LDPC)

This Forward Error Correction (FEC) encoding sub-module takes a baseband frame as input. Firstly, it performs outer coding on this baseband frame by Bose-Chaudhuri-Hocquengham (BCH) encoding and produces a set of bits called BCHFEC, which is then added at the end of the baseband frame. Then it performs inner encoding on this modified baseband frame by Low Density Parity Check (LDPC) encoding and produces a set of bits called LDPCFEC, which is later appended at the end of the modified baseband frame, as presented in Figure 3.3.

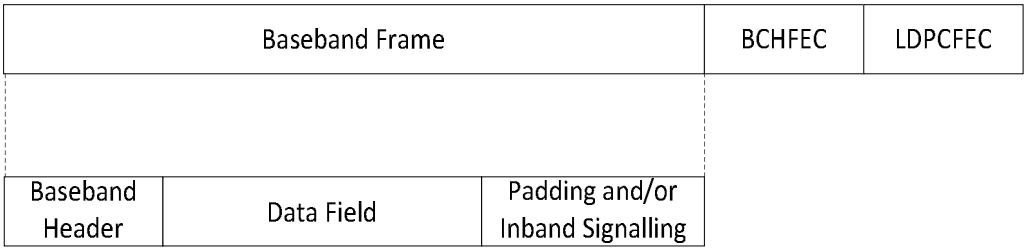

Figure 3.3. *DVB-T2 data format before bit interleaving [4].*

3.4.3.2 Bit interleaver

Bit interleaver sub-module performs bit interleaving on the output frame produced by LDPC encoder. This bit interleaving is done in two parts. At first, only parity bits are interleaved and at last, all the bits are column-twist interleaved. Column-twist interleaving means that bits are written column-wise, with write position for each column is twisted little, and later bits are read row-wise.

3.4.3.3 Demux bits to cells

After bit interleaving, this sub-module de-multiplexes all the bits into parallel cells so that later these cells can be mapped into constellation points.

3.4.3.4 Mapper

The mapper sub-module maps the cell words into constellation points. The available modulations are QPSK, 16-QAM, 64-QAM and 256-QAM.

3.4.3.5 Constellation rotation and cyclic Q-delay

This is an optional sub-module that rotates the constellation points of each cell in the complex plane and then cyclically delays the imaginary part by one cell. The angle of

rotation is different for different modulation as it depends on the modulation chosen. However, if this sub-module is not used, then the cells are kept unmodified and passed from mapper to cell interleaver.

3.4.4 Frame mapper

Frame mapper module consists of cell interleaver, time interleaver, frame builder and frequency interleaver. It takes input from BICM module and produces output for modulator module.

3.4.4.1 Cell interleaver

Cell interleaver sub-module interleaves the cells of each FEC block by employing a pseudo-random permutation. It uses different pseudo-random permutation for different FEC blocks in order to maintain uncorrelated distribution of channel distortions and interferences for the FEC blocks in the receiver. Moreover, cell interleaver increases the separation between cells if rotated constellations are used.

3.4.4.2 Time interleaver

The purpose of time interleaver is to spread the cells of each FEC block over many symbols and over many different T2 frames in order to tolerate time varying channels and impulsive interference. Incoming cells are written column-wise in the interleaver memory. When all the cells of all the FEC blocks are written, then the interleaving frame is divided into time-interleaver blocks, which are later read row-wise.

3.4.4.3 Frame builder

Frame builder assembles the cells produced by time interleaver for each of the PLPs into OFDM symbols according to scheduling information of scheduler and configuration of the frame structure. It also organizes the cells of the modulated L1 signalling data.

3.4.4.3.1 Frame structure

A DVB-T2 super frame is composed of many T2 frames in the hierarchical structure. Each of the T2 frame starts with a P1 symbol, followed by a number of P2 symbols for the L1 signalling block, followed by the data symbols. The structure of the DVB-T2 frame is given in Figure 3.4.

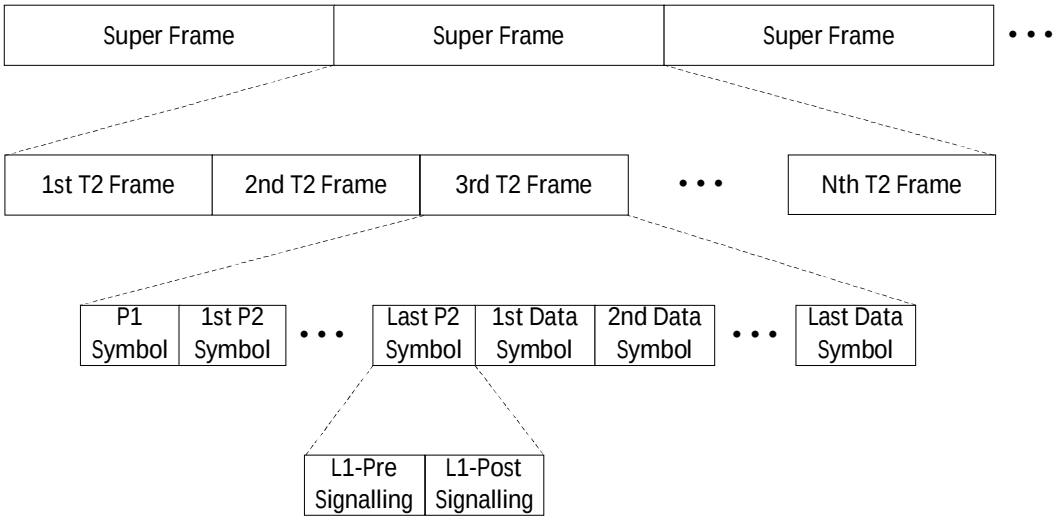

Figure 3.4. *DVB-T2 frame structure [4].*

3.4.4.3.2 Insertion of preamble symbols

Frame builder inserts the preamble P1 and P2 symbols whereas P1 symbol is the first preamble symbol that also marks the start of the frame.

3.4.4.3.3 P1 symbol

A dedicated P1 symbol preamble is used in DVB-T2 at the beginning of every OFDM data frame so that the receiver can promptly identify and decide the presence of DVB-T2 signal in the radio frequency channel and can achieve correct coarse symbol and fine frequency synchronization. In addition, some parameters like FFT mode of the transmission, Single Input Single Output (SISO) / Multiple Input Single Output (MISO) and presence or absence of Future Extension Frame (FEF) are signaled by P1 symbol. Furthermore, when the receiver is tuned to the nominal frequency, then it does not need to test all the frequency offsets individually as any amount of frequency offset can be detected.

3.4.4.3.4 P2 symbol

A number of P2 symbols follow the P1 symbol in every OFDM frame whose main purpose is to carry L1 signalling data that provides the receiver a way to access the PLPs within the T2 frames. The L1 signalling data is divided into L1-pre and L1-post signalling where L1-pre signalling enables the receiver to receive and decode L1-post signalling. This L1-post signalling conveys the needed parameters to the receiver in order to access the PLPs. There may be more than one P2 symbols in each DVB-T2 frame and this number is fixed for a particular FFT size.

3.4.4.3.5 Frequency interleaver

The frequency interleaver is a pseudo-random block interleaver operating on OFDM symbols that takes the data cells from the frame builder and mixes them. Instead of working like the other interleavers that works on single PLP, frequency interleaver mixes the cells coming from different PLPs carried out in the same OFDM symbol. Furthermore, it also employs a pseudo-random permutation on the output of the time interleaver in order to disrupt the structured nature so that consecutive symbols will be transmitted in different frequencies and therefore they will be more tolerant to regular error bursts in the transmission channel.

3.4.5 Modulator

The modulator module is comprised of MISO processing, pilot insertion, IFFT, PAPR reduction, guard interval insertion, P1 symbol insertion and D/A converter sub-modules that are briefly described in the following subsections.

3.4.5.1 MISO processing

When MISO processing is applied on the cell level to the symbols of DVB-T2 signal, then this sub-module takes the input cells and produces two similar sets of data cells by using a modified Alamouti based encoding. Afterwards, these two sets of data cells are directed to two groups of transmitters. However, this Alamouti based encoding is not applied to the preamble symbol P1 and to the pilots.

3.4.5.2 Pilot insertion

A pilot refers to a cell within the OFDM frame which is modulated with predefined reference information that is also known to the receiver and transmitted at boosted power level. The location and number of the pilots are defined in the standard and the value of the pilots are derived from a reference sequence which is applied to all the pilots of different types, namely, scattered pilots, continual pilots, edge pilots, P2 pilots and frame closing pilots. However, the phases of scattered, continual and edge pilots are modified for different transmitters if MISO mode is used.

3.4.5.3 IFFT

Since OFDM is used as the modulation technique in DVB-T2 system, so this sub-module performs IFFT in the transmitter to convert the signal from frequency domain to time domain.

3.4.5.4 PAPR reduction

DVB-T2 presents two techniques for reducing PAPR, namely Active Constellation Extension (ACE) and Tone Reservation (TR) techniques. The presence or absence of one or both of these techniques is signaled in L1 signalling. However, these techniques are applied on the other parts of each OFDM symbol except P1 symbol.

3.4.5.5 Guard interval insertion

Guard interval is the cyclic continuation of the useful part of the symbol that is inserted at the beginning before the useful part of every OFDM symbol. This sub-module inserts one of the guard interval fractions among the seven different choices available for each FFT size in DVB-T2.

3.5 Key Differences between DVB-T2 and DVB-T

This subsection focuses on the fundamental technological differences between DVB-T2 and DVB-T. Significant improvements of the new DVB-T2 specification compared to DVB-T include new error correction strategy, high order modulation modes, reduced overhead of pilots and inclusion of preambles for enhancing signal detection and synchronization. Furthermore, it also has more options for number of carriers, bandwidth, guard interval and pilot pattern based on the need of the channel [19].

DVB-T2 introduces fully transparent PLP, where each PLP can have data with different structures and independent parameters. For example, the parameters like constellation, code rate or the time-interleaving depth may be different for different PLPs. Moreover, two input modes are defined: input mode A for single PLP and input mode B for multiple PLPs in order to use this type of multiple PLP service.

DVB-T2 gives more options for bandwidth selection as it includes two more options with the previous options for DVB-T. The newer standard has a 10 MHz bandwidth option for professional use and a 1.712 MHz option for mobile services with the previous 6 MHz, 7 MHz and 8 MHz options compared to DVB-T. Also the highest order of constellation available in DVB-T2 is 256-QAM whereas it is 64-QAM for DVB-T. Using a high order constellation will increase the capacity and efficiency.

The choice for number of carriers is more increased in DVB-T2 as it has six options for FFT-size: 1k, 2k, 4k, 8k, 16k and 32k, while DVB-T has only two options: 2k and 8k. When FFT-size is increased, then better robustness against impulsive noise can be achieved and guard interval overhead for a particular symbol will be reduced. Furthermore, there is another possibility in DVB-T2 standard to increase the number of subcarriers per symbol for data transport by using an extended carrier mode for 8k, 16k and 32k FFT-size options. In this extended carrier mode, the outer end of the OFDM signal spectrum can be extended because the rectangular part of the spectrum rolls off more quickly for higher FFT-size options.

DVB-T2 transmits preamble symbols with signalling data in the beginning of the physical layer frame in order to indicate the transmission type and basic transmission parameters in a robust way. For instance, every DVB-T2 frame starts with a P1 symbol preamble to detect the presence of a DVB-T2 signal, to achieve synchronization faster and to disclose the FFT-mode and SISO/MISO mode of the transmission. Moreover, a number of P2 symbols are present as a preamble in order to carry all static, configurable and dynamic layer-1 signalling. On the other hand, DVB-T does not have any preamble symbols.

The new DVB-T2 standard has more flexible options for scattered pilots that can be used based on the chosen FFT-size and guard interval fraction, while the old DVB-T standard has a fixed static pilot pattern. Therefore selecting a scattered pilot pattern depending on the FFT-size and guard interval fraction will reduce the overhead for carrying the pilots. In addition, the overhead for continual pilots are also reduced in DVB-T2.

DVB-T2 presents a new technique where the constellation is rotated in the complex I/Q plane in order to associate enough information so that each axis on its own can determine which point was sent. Moreover, the I and Q components are transmitted on different frequencies at different times as they are separated by the interleaving process. This results in a situation where if one component is destroyed by the channel, then the other component can be used to recover the destroyed component.

A significant amount of performance enhancement is possible in DVB-T2 as it has four interleavers, namely, bit, cell, time and frequency interleavers. The goal of the interleavers is to spread the data in both time and frequency domain in such a way

that long sequence of data will not be destroyed by impulsive noise or frequency-selective fading. Impulsive noise is characterized as disturbance over a short time period and frequency-selective fading is characterized as disturbance over a limited frequency span. Moreover, the time interleaver also protects the DVB-T2 signal against time-selective fading.

DVB-T2 uses LDPC combined with BCH coding that offers excellent performance in the presence of high noise level and interference. Therefore better error protection is expected in DVB-T2 compared to DVB-T as the latter one uses convolutional and Reed-Solomon codes. In addition, PAPR is another important factor in OFDM systems as high PAPR can reduce the efficiency of the power amplifier. Therefore, DVB-T2 has two strategies to reduce the PAPR described earlier. Furthermore, DVB-T2 has an option of FEF in order to be able to include future advancement in the standard.

The differences between DVB-T and DVB-T2 are summarized in Table 3.1.

Subject	DVB-T	DVB-T2
PLP	Not present	Present
Bandwidth	6 MHz, 7 MHz, 8 MHz	1 MHz, 6 MHz, 7 MHz, 8 MHz, 10 MHz
Constellation mode	QPSK, 16-QAM, 64-QAM	QPSK, 16-QAM, 64-QAM, 256-QAM
Carriers	2k, 8k	1k, 2k, 4k, 8k, 16k, 32k
Preambles (P1 & P2)	Not present	Present
Scattered Pilots overhead	8% of total	1%, 2%, 4%, 8% of total
Continual Pilots overhead	2.6% of total	0.35% of total
Constellation rotation	Not present	Present
Interleavers	Outer and inner interleavers	Bit, Cell, Time and Frequency interleavers
FEC encoding and code rate	Reed Solomon + Convolutional 1/2, 2/3, 3/4, 5/6, 7/8	LDPC + BCH 1/2, 3/5, 2/3, 3/4, 4/5, 5/6
Guard Interval	1/4, 1/8, 1/16, 1/32	1/4, 19/256, 1/8, 19/128, 1/16, 1/32, 1/128
PAPR reduction	Not present	ACR and TR techniques
FEF	Not present	Present

Table 3.1. *Comparison summary between DVB-T and DVB-T2 [20].*

4. Channel models

The propagation effects and related signal impairments during transmission are often collected and categorically denoted as channel. Channel modeling is one of the essential elements of the simulation chain and it is heavily dependent on the radio propagation environment. It is also an important requirement for assessing technology for wireless systems. This chapter offers a brief overview about signal propagation and channel parameters along with wireless channel models that have been used in performance evaluation.

4.1 Radio propagation environment

The transmitter transmits the signal by its antenna that propagates through the wireless radio propagation environment and is received by the antenna of the receiver. However, this wireless channel may have many obstacles that may cause the signal to attenuate, reflect, diffract or scatter before arriving at the receiver. Therefore the received signal may be a combination of many replicas of the original signal impinging at receiver from many different paths. The component signals on these different paths can have constructive or destructive interference with each other and this phenomenon is referred as multipath propagation [21]. The received signals may be diversely delayed, attenuated and their phase, arrival angle may vary because of the presence of multiple paths [22].

The radio propagation phenomena will be time varying and fading will occur if either the transmitter or the receiver is moving. Fading introduces periods of low SNR that leads to burst error during transmission [23]. Moreover, signal pulses will be

broadened as different paths will have different travel time. This restricts the maximum information rate of the wireless system at which adjacent signal pulses can be transmitted without overlapping. Furthermore, this spreading of the signal in time domain leads to ISI and results in transmission burst error [23].

The quality of the received signal depends on the propagation channel. In an optimal transmission channel, there is only a direct Line-Of-Sight (LOS) path between the transmitter and the receiver. This means that the signal arrives straight to the receiver via the shortest possible path without any reflections. However, if the receiver is behind an obstacle or inside a building, the LOS path may be absent and the arriving signal can be diffracted, reflected, or scattered. This situation is known as Non-LOS (NLOS) scenario [24] [25].

4.2 Channel parameters

The wireless channel is characterized by several parameters like multipath delay spread, Doppler spread, coherence bandwidth, coherence time and fading characteristics. Therefore these parameters are discussed in the following subsections.

4.2.1 Delay Spread

The received signal has a longer duration than the transmitted signal because of the different delays of different propagation paths. The time difference between the first multipath, i.e., the LOS component and the last one is called delay spread. This phenomenon is also referred as time dispersion of the signal. It can cause overlapping of the data symbols that leads to bit errors [23].

Suppose that a very narrow pulse is transmitted in a fading channel. Then the received power can be measured as a function of time delay. The average received power $P(\tau_e)$ as a function of the excess time delay (τ_e) is called the multipath intensity profile or the delay power spectrum. Excess time delay is the difference between total time delay and time delay of the first path. The range of values of τ_e over which $P(\tau_e)$ is essentially non-zero is called the multipath delay spread of the channel, and is often denoted by T_m. It essentially tells the maximum delay between paths of significant power in the channel.

4.2.2 Doppler Shift and Doppler Spread

The movement of the receiver with respect to the transmitter introduces some frequency shift to the received signal. This is called Doppler effect and the frequency shift is known as Doppler shift, represented by f_d. Besides, the received signal has a larger bandwidth than the transmitted signal because of the different Doppler shifts introduced by the multipath components and receiver speed [23]. This phenomenon is referred as frequency dispersion and the possible range of the Doppler shift is defined as Doppler spread, denoted by $(\Delta f)_{ds}$.

4.2.3 Coherence Bandwidth

Coherence bandwidth of the channel is a measure of the maximum bandwidth or frequency interval over which two frequencies of a signal are likely to experience comparable or correlated amplitude fading. It means that the frequency components separated by a frequency interval greater than the coherence bandwidth are distorted in an uncorrelated manner. In other words, maximum transmission bandwidth over which the channel can be assumed to be approximately constant in frequency can be referred as coherence bandwidth, denoted by $(\Delta f)_c$. Coherence bandwidth helps to understand whether the channel is frequency flat or frequency selective. Multipath delay spread (T_m) is inversely proportional to coherence bandwidth $(\Delta f)_c$ [26].

4.2.4 Coherence Time

The impulse response of a channel varies with time in a time-varying channel. The coherence time, denoted by $(\Delta t)_c$, gives a measure of the time duration over which the channel impulse response is highly correlated. As a result, the channel can be considered as time invariant during the reception of a symbol if the symbol duration is smaller than coherence time [27]. Based on the measure of the coherence time, it is possible to determine whether the time variant channel can be considered as fast or slow fading channel. It can be shown that Doppler spread $(\Delta f)_{ds}$ is inversely proportional to coherence time $(\Delta t)_c$ [26].

4.2.5 Fading with classification

Fading is the deviation of the transmitted signal over certain transmission channel. It is caused by the constructive or destructive interference between two or more replicas of the transmitted signals that traverse through different paths and arrive at the receiver at slightly different times. The amplitude or the phase of the resultant

received signal may vary depending on several factors like intensity, relative propagation time and bandwidth of the transmitted signal [21].

Whenever fading, i.e., the fluctuations in the envelope of the transmitted radio signal is considered, then the observation duration should also be taken into account to indicate whether the duration is over short or long distance. If the observation duration is over short duration for a wireless channel, then rapid fluctuations can be found in the signal envelope. On the other hand, a slowly varying averaged view can be found for long observation duration. Therefore, the former scenario is referred as small-scale or multipath fading and the latter scenario is referred as large-scale fading or path loss [23] [28]. Large scale fading or path loss is characterized by the gradual loss of the received signal strength since the signal propagates in all directions to cover the distance from the transmitter to the receiver.

Multipath fading or small scale fading is characterized by the fact that the instantaneous received signal power is a sum of many contributors coming from different multipaths reaching the receiver. This sum of the contributions varies widely as the phases are random [28]. However, small-scale fading can be classified by the following types, namely, flat fading, frequency selective fading, fast fading and slow fading.

4.2.5.1 Flat fading

Flat fading happens when the bandwidth of the transmitted signal is much smaller than the coherence bandwidth of the channel. In other words, the channel is characterized as flat fading channel if it experiences constant gain and linear phase response over a bandwidth greater than the bandwidth of the transmitted signal [29]. Moreover, the spectral characteristics of the transmitted signal are maintained in this type of fading channel. However, the strength of the received signal changes with time because of the fluctuations caused by multipath. In addition, the multipath delay spread remains smaller than the symbol period for flat fading.

4.2.5.2 Frequency selective fading

A channel is said to be frequency selective if the bandwidth of the transmitted signal is greater than the coherence bandwidth of the channel and the multipath delay spread is also greater than the symbol period. In the case of frequency selective fading, different frequencies of the transmitted signal experience different extent of fading and do not retain their original phases and relative amplitudes. As a result, this type of fading

causes massive distortion to the signal. However, DVB-T2 uses OFDM that tries to solve this problem by dividing the channel bandwidth into sub-carriers, each of which can be individually transmitted in a frequency flat manner when the channel is frequency selective [29].

4.2.5.3 Fast fading

Fast fading happens if the received signal level has rapid fluctuations. In another words, fast fading occurs when coherence time of the channel is smaller than symbol period of the transmitted signal [26]. This condition causes the channel to be time selective or time-variant. Furthermore, in the case of fast fading, the Doppler spread of the channel is greater than the bandwidth of the baseband signal. Fast fading happens because of the reflections of local objects and the motion of the receiver relative to those objects [29].

4.2.5.4 Slow fading

Slow fading occurs when coherence time of the channel is much greater than symbol period of the transmitted signal. If this condition holds, then the channel is referred as time flat or time-invariant channel [29]. However, the Doppler spread of the channel is much smaller than the bandwidth of the baseband signal in the case of slow fading.

4.3 Channel

To analyze the synchronization performance of DVB-T2 system, the simulation model has to be evaluated in different channel models. This section presents a brief overview of the channel models that have been used for assessing the performance of the DVB-T2 system.

4.3.1 Gaussian Channel

The behavior of a typical wireless fading channel is considerably more complex to deal with than a Gaussian channel that models the noise generated at the receiver front end in the case of ideal transmission channel. The noise is assumed to have a Gaussian probability distribution function and a constant power spectral density over the channel bandwidth [23]. Hence it is often referred as Additive White Gaussian Noise (AWGN) channel. It provides a considerably useful model for direct LOS path between single transmitter and single receiver channels [21].

4.3.2 Static Channel

The static channels that have been used in the evaluation of the DVB-T2 receiver performance are mainly Ricean channel and Rayleigh channel. A brief of description of these channels are given here.

4.3.2.1 Ricean Channel

Ricean fading channel has at least one strong dominant LOS signal path along with several weaker NLOS paths [30]. This dominant path is responsible to reduce the delay spread and to decrease the fading depth. In addition, the envelope of the received signal is statistically described by a Ricean probability density function; hence it is referred as Ricean channel [23].

The Ricean fading channel, defined in DVB-T specification, is used for describing the fixed, outdoor rooftop-antenna reception condition for DVB-T2 systems as well [19]. This channel model does not include any Doppler and should therefore be considered as a snapshot of the real time-variant channel. The model is defined by the following equation where *x(t)* and *y(t)* are input and output respectively [19].

$$y(t) = \frac{\rho_0 x(t) + \sum_{i=1}^{N} \rho_i e^{-j\theta_i} x(t-\tau_i)}{\sqrt{\sum_{i=0}^{N} \rho_i^2}} \qquad (4.1)$$

where ρ_0 represents the line of sight ray, N is the number of echoes except the LOS, θ_i is the phase shift from scattering of the ith path, ρ_i is the attenuation of the ith path and τ_i is the relative delay of the ith path. The phases, delays and attenuations are defined in [19]. The Ricean factor K, that is, the ratio of the power of the direct path to the reflected paths, is given as

$$K = \frac{\rho_0^2}{\sum_{i=1}^{N} \rho_i^2} \qquad (4.2)$$

In the simulations, a Ricean factor K = 10 has been used. It refers to fixed reception according to the specification. Figure 4.1 presents the average impulse response and average frequency response for Ricean channel.

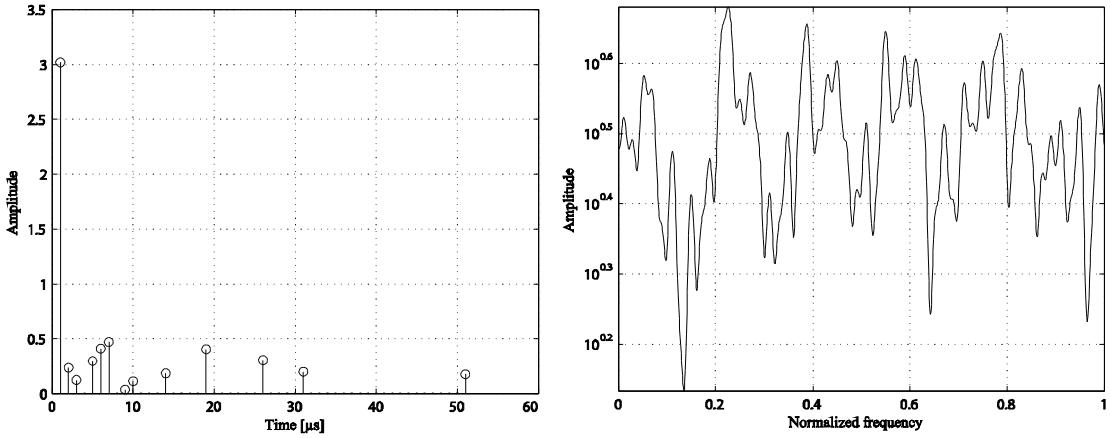

(a) (b)

Figure 4.1. *a) Average impulse response and b) Average frequency response for Ricean channel.*

4.3.2.2 Rayleigh Channel

Rayleigh fading channel assumes that all paths are relatively equal and there is no dominant LOS path. It is a reasonable model that considers many objects in the environment that scatter the radio signal before it arrives at the receiver. Moreover, the probability density function of the received signal envelope is characterized by Rayleigh distribution. Therefore, it is referred as Rayleigh channel model [22]. Rayleigh fading is more severe than Ricean fading as the fading fluctuations are deeper in the former one [25].

The Rayleigh fading channel is used for describing the portable indoor or outdoor reception condition for DVB-T2, which was first defined for DVB-T Specification [19]. This channel model does not include any Doppler and therefore, should be considered as a snapshot of the real time-variant Rayleigh channel. The model is defined by the following equation where *x(t)* and *y(t)* are input and output respectively [19].

$$y(t) = k\sum_{i=1}^{N} \rho_i e^{-j\theta_i} x(t-\tau_i) \qquad (4.3)$$

where ρ_i is the attenuation of the *i*th path, θ_i is the phase shift from scattering of the *i*th path, τ_i is the relative delay of the *i*th path, and *k* is defined as

$$k = \frac{1}{\sum_{i=1}^{N} \rho_i^2} \qquad (4.4)$$

It means that the line of sight parameter (ρ_0) is zero for Rayleigh channel model. It refers to portable reception according to the specification. The average impulse response and average frequency response of Rayleigh channel is presented in Figure 4.2.

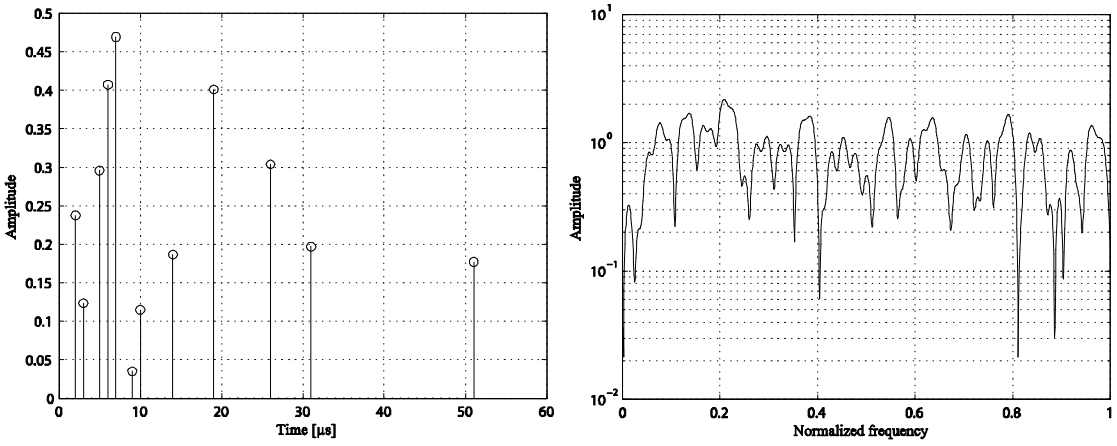

(a) (b)

Figure 4.2. *a) Average impulse response and b) Average frequency response for Rayleigh channel.*

4.3.3 Mobile Channel

Mobile channel modeling is challenging as the receiver speed, path delay, gain and signal arrival angle are always changing. The mobile channel that has been used to evaluate the system is typical urban (TU6) channel. The TU6 channel model is defined by the EU COST 207 project [31].

It got its name as TU6 as it models the terrestrial propagation in an urban area by using 6 resolvable paths having wide dispersion in delay and relatively strong power. Many simulation results in this thesis are evaluated in TU6 channel, though it is not totally applicable for handheld application. The TU6 channel profile parameters are given in Table 4.1 [19].

Tap number	Delay (μs)	Power (dB)	Power (Linear)	Doppler Spectrum
1	0	-3	0.5	Classical
2	0.2	0	1	Classical
3	0.5	-2	0.63	Classical
4	1.6	-6	0.25	Classical
5	2.3	-8	0.16	Classical
6	5.0	10	0.1	Classical

Table 4.1. *Typical urban (TU6) channel profile.*

Where the classical Doppler spectrum is defined as [19]:

$$S(f, f_D) = \frac{1}{\sqrt{1-(f - f_D)^2}} \qquad (4.5)$$

The TU6 channel model is illustrated by the average impulse response and average frequency response given in Figure 4.3.

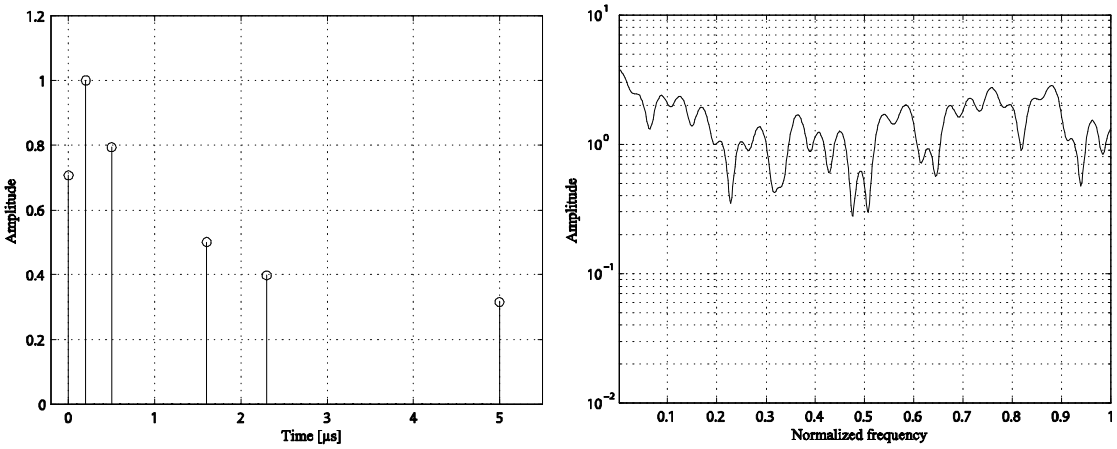

(a) (b)

Figure 4.3. *a) Average impulse response and b) Average frequency response for TU6 channel.*

4.3.4 SFN Channel

In Single Frequency Network (SFN) channel model, several transmitters located in different locations synchronously transmit identical signal on the same frequency. As a result, the receivers will receive the superposition of signals coming from different

transmitters with different delays. Therefore the guard interval should be large enough to mitigate ISI [32]. SFN can provide a large coverage area by using only single frequency, thus showing high frequency efficiency and less interference compared to Multi Frequency Network (MFN). Moreover, there will be no single point of failure if one transmitter fails to transmit since the receiver is likely to receive the same signal from other transmitters because of overlapping coverage [33]. Furthermore, SFN can use transmitters with lower power and be more cost effective. SFN also makes portable reception easier as the frequency is same in the coverage area, so there will be no need of handovers.

The SFN channel profile has been implemented by including only Rayleigh paths. It means that two Rayleigh channels are modeled with a delay in between them. Figure 4.4(a) presents the average impulse response of an SFN configuration with two Rayleigh channels with a delay of 128 µs in between them. Also the average frequency response is given in Figure 4.4(b).

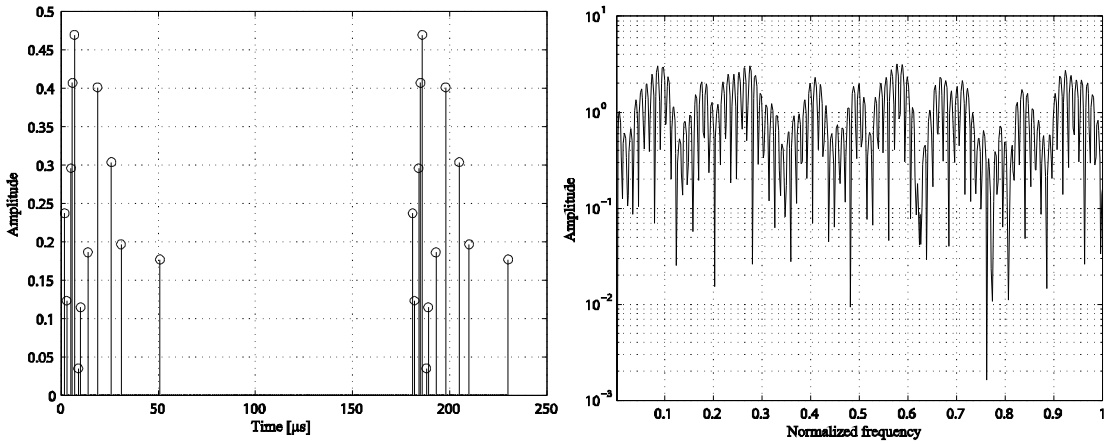

(a) (b)

Figure 4.4. *a) Average impulse response and b) Average frequency response for SFN channel.*

5. Synchronization schemes

Synchronization is an important issue in DVB-T2 as the receiver needs to locate the signal in both time and frequency before it can extract the transmitted information. After achieving synchronization, it must be tracked continuously throughout the reception process. DVB-T2 uses OFDM as its modulation technique and OFDM systems are very sensitive to both symbol timing and frequency errors [34]. This chapter deals with the features defined in DVB-T2 in order to achieve synchronization, for example, P1 symbol, P2 symbol and scattered and continual pilots. Mainly the synchronization features that can be achieved by P1 symbol is considered in this thesis.

5.1 Overview of synchronization in OFDM

Synchronization is a very important issue in systems like DVB-T and DVB-T2 that uses OFDM, because lack of synchronization will be responsible for ISI and ICI [6]. Every OFDM system has to deal with the following three synchronization issues: symbol synchronization, frequency synchronization and sampling clock synchronization.

5.1.1 Symbol synchronization

Whenever signals are transmitted through severe channel conditions in the presence of multipath fading, phase noise and Doppler shift, then symbol synchronization is a must in the receiver in order to correctly receive the transmitted symbols [34]. At the beginning of the reception, the receiver has no idea about the symbol positions. Hence

it has to obtain the correct symbol timing as soon as possible so that frequency synchronization and channel estimation can take place.

The target of symbol timing synchronization is to determine the correct starting position of the symbols in the time domain in order to perform demodulation correctly [6]. If the estimation of the FFT-window is within the guard interval, then the OFDM symbols will not be affected by ISI and the phase rotation caused by timing offset can be easily corrected after FFT. Otherwise if the FFT-window is misplaced, then ISI will be introduced, meaning that, the sampled OFDM symbol will contain some samples belonging to other symbols. This will cause the dispersion of signal constellation and consequently, the system performance will be decreased [34].

Symbol synchronization can be carried out either by data-aided or non-data-aided approach. In data-aided approach, pilot sequences are used that are known to the receiver. However, in non-data-aided approach, the receiver makes an attempt to find out the symbol starting position based on the signal statistics. Besides, symbol synchronization is performed in two stages: coarse symbol synchronization is performed before FFT and fine symbol synchronization is performed after FFT [35]. The goal of coarse symbol synchronization is to find out accurate enough FFT-window position in the time domain and it is achieved mainly by non-data-aided approach, like guard interval correlation or maximum-likelihood algorithms [36]. On the other hand, fine symbol synchronization is performed in frequency domain after performing the FFT operation to achieve a more accurate estimation and it can be carried out by data-aided approach using the pilots, especially scattered pilots [35].

5.1.2 Carrier frequency synchronization

Frequency synchronization is needed in order to protect the system from ICI and maintain the orthogonality of the subcarriers in the OFDM symbol. Orthogonality can be destroyed in the presence of carrier frequency offset, which occurs when the local oscillator of the transmitter and the receiver are not synchronized. Further offset can be introduced by the relative motion of transmitter and receiver, known as Doppler spread [34].

The carriers in OFDM are inherently closely spaced in frequency compared to the channel bandwidth. Therefore OFDM can tolerate frequency offset that is a very small fraction of the channel bandwidth. However, carrier frequency offset has two

parts – one fractional part and one integer part. The fractional or fine part of the frequency offset is less than half subcarrier spacing and is responsible for reduction of the signal amplitude in the output and ICI, resulting in a performance degradation of the receiver. On the other hand, the integer part of the frequency offset is an integer multiple of the subcarrier spacing and is responsible for a constant amount of shift of the subcarrier indices that results in a rotation of the constellation [37].

Furthermore, frequency synchronization can be divided into pre-FFT and post-FFT stages. Non-data-aided pre-FFT algorithms can be used to quickly determine the fractional part of the frequency offset but these algorithms are not able to determine the integer part. On the other hand, data-aided pilot based post-FFT algorithms can be used to determine the integer part of the frequency offset. After determining the fractional and integer part, post-FFT data-aided tracking is carried out in order to maintain orthogonality [38].

5.1.3 Sampling clock synchronization

Whenever the sampling clocks of the transmitter and the receiver are not synchronized, then there will be an offset called sampling clock offset. The generation of this offset can be contributed by other factors like multipath fading, noise and symbol timing estimation error. The sampling clock offset is divided in two parts: the sampling phase offset and the sampling frequency offset [34].

The sampling phase offset will lead to signal phase distortion. On the other hand, sampling frequency offset, i.e., the difference in the sampling frequencies in the transmitter and the receiver will lead to a continuous drifting of the sampling time instant. If this sampling frequency offset is not estimated and mitigated afterwards, then some amount of ICI will be introduced [34]. However, this sampling clock synchronization is not considered in this thesis.

5.2 Synchronization in DVB-T

Synchronization algorithms for DVB-T system can be classified in two major categories. One category exploits the cyclic extension structure of the OFDM symbol, while the other category uses algorithms to exploit the pilots in order to achieve synchronization [39]. DVB-T system has scattered pilots, continual pilots and transmitter parameter signalling (TPS) carriers in order to carry out the aforementioned synchronization tasks [2].

The synchronization methods in DVB-T that uses cyclic extension structure are able to perform both the detection of the beginning of the OFDM symbol and the correction of frequency offset [36]. However, in multipath channels, these methods only provide coarse symbol synchronization, which is needed to be refined further later. DVB-T can use continual and scattered pilots in order to perform the fine symbol and coarse frequency synchronization [35].

Moreover, TPS carries some fixed number of bits that carries information in order to maintain synchronization. The TPS block in DVB-T standard is defined over one OFDM frame of 68 consecutive OFDM symbols where each symbol contributes one TPS bit to the TPS block. The TPS is transmitted in parallel on 17 carriers in 2k mode and on 68 carriers in 8k mode. However, every TPS carrier in the same symbol conveys the same differentially encoded information bit. Each TPS block in DVB-T carries 16 synchronization bits within its total 68 bits. Since there can be four OFDM frames within an OFDM super frame, therefore there are two sequences for the 16 synchronization bits: one for first and third TPS block and another one for second and fourth TPS block in a super frame [2].

5.3 Synchronization in DVB-T2

Synchronization is very important in DVB-T2 system and the receiver has to perform synchronization tasks before starting the demodulation of the subcarriers. Firstly, the receiver has to obtain correct symbol timing in order to minimize the effects of ISI and ICI. Secondly, it has to determine and correct the carrier frequency offset of the received signal to remove the ICI [6]. To deal with different synchronization tasks, DVB-T2 system has different signal features, like P1 symbol, P2 symbol and scattered and continual pilots [4]. Synchronization schemes in DVB-T2 also have to deal with clock synchronization. However, this thesis focuses on the synchronization schemes that can be achieved by using P1 symbol. Therefore, clock synchronization is out of the scope of this thesis.

At the beginning, the receiver starts the scanning process without any knowledge of the channel or the signal. Whenever the receiver finds a P1 symbol, then it can deduce the presence of T2 signal in the channel. After that, the receiver uses P1 symbol to perform some symbol and frequency related synchronization and can determine the FFT size. Once the receiver knows the FFT size, then it can move forward to deduce the guard interval. To know further information about the pilot

patterns used in the main payload, the receiver needs to decode the L1 signalling in P2 symbol(s). Since the receiver knows the FFT size at this stage, so it can deduce the P2 pilot patterns used and thus able to decode P2 and L1 data. By decoding the L1 signalling information, the receiver knows the pilot pattern and guard interval of the data symbols [19].

5.3.1 Synchronization using P1 symbol

According to the frame structure of DVB-T2, every T2 frame has a P1 symbol at the very beginning. After that P1 symbol, there will be one or more P2 symbol(s) before the data symbols. Figure 5.1 shows the position of the P1 symbol in the DVB-T2 frame.

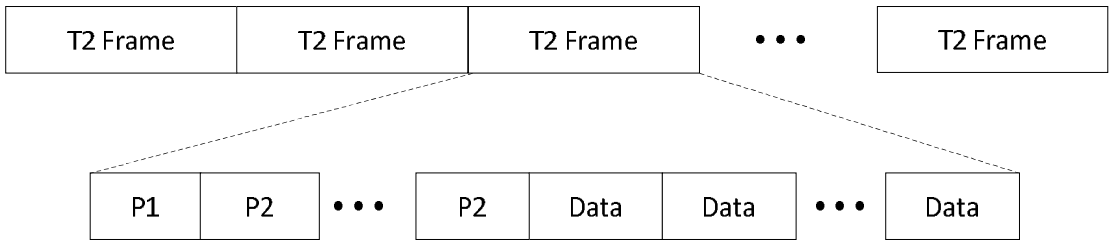

Figure 5.1. *Position of P1 symbol in DVB-T2 frame.*

5.3.1.1 P1 symbol overview

P1 symbol preamble is inserted only once at the beginning of every T2-frame in order to announce the beginning of each T2 frame and FEF part. According to the standard [4], P1 symbol enables the receiver to determine the presence of T2 signal very quickly during the initial signal scan phase. Recognition of the P1 symbol is enough to conclude that the particular RF channel carries DVB-T2 signal. Moreover, it identifies the preamble itself as a T2 preamble as a signal may contain both T2 frames and FEF parts.

Furthermore, P1 symbol discloses some basic transmission parameters that are needed to decode the rest of the preamble and subsequently the main payload. Mainly it discloses the FFT mode of the transmission and tells whether the transmission is SISO or MISO. In addition, the receiver can use P1 symbol to detect and correct timing and frequency synchronization. Therefore, P1 symbol saves time during the scanning and channel setup process and helps to achieve synchronization [4].

5.3.1.2 P1 symbol evolution

P1 symbol is a completely new concept for DVB-T2 and it was not present in DVB-T. Therefore, the P1 preamble symbol structure and the corresponding receiver processing chain in the standard went through some development phases before finalizing in the DVB-T2 standard. The following subsections give a brief idea about the evolution of the P1 symbol structure and the corresponding receiver processing chain. It also discusses the capabilities and drawbacks of each one that motivates to develop a new structure to overcome the drawbacks of the previous one.

5.3.1.2.1 A-B structure

The first proposal for P1 symbol was to insert a unique signal discovery symbol at the beginning of every T2 frame. It is an OFDM symbol that certainly has its guard interval extension, and will essentially have different characteristics than the other data symbols. Thus it would have been enough for the receiver to look for this special symbol in order to declare signal discovery.

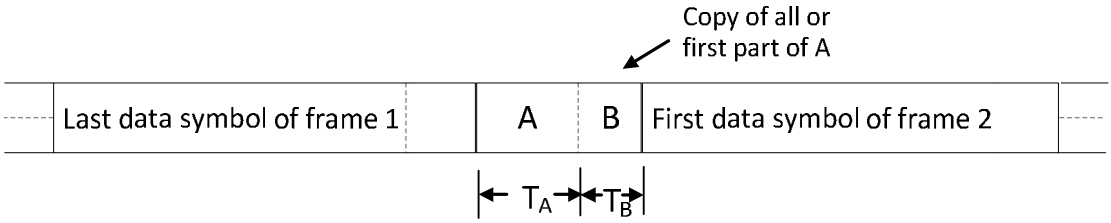

Figure 5.2. *P1 symbol, A-B structure.*

Figure 5.2 shows the structure and position of P1 symbol that has two parts, namely part A and part B with duration T_A and T_B respectively. This P1 symbol is placed after the last data symbol of the previous T2 frame and just before the first data symbol of the next T2 frame. Here, part B is the guard interval that can be same as part A, or can be a copy from the beginning of part A, or can have many complete repetitions of part A.

The first phase in the receiver processing is signal discovery, meaning that, the receiver has to detect the presence of its desired signal as quickly as possible during the searching in some particular RF channel despite the presence of frequency offset. The well known guard interval correlation method described in [36] can be used for the detection purpose as the P1 symbol has guard interval extensions. The presence of guard interval ensures strong correlation between points in the OFDM symbol that are separated by FFT length.

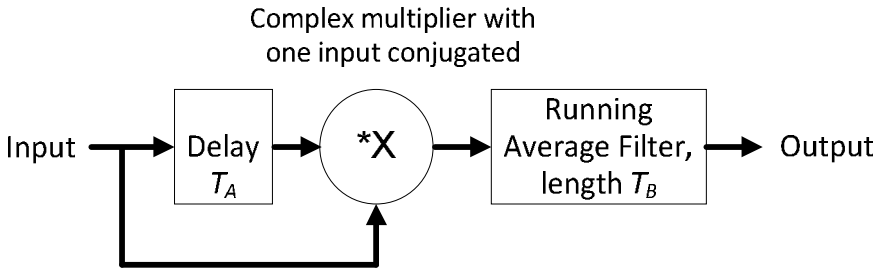

Figure 5.3. *Receiver processing chain for A-B structure.*

The receiver processing chain is shown in Figure 5.3 [40]. The received signal is delayed by T_A and then multiplied with the original received signal after taking the complex conjugation of one of them. This multiplication is later filtered to reduce the degree of noisiness. For example, a running average filter of same length as the guard interval can be chosen. The output of this receiver processing chain will give a triangular output pulse indicating the start of a frame, and whose magnitude corresponds to the presence of every P1 symbol and argument corresponds to the frequency offset.

However, this simple A-B structure for P1 symbol has few drawbacks, like false detection, Continuous Wave (CW) interferers and dangerous delays. For false detection case, the problem is that the guard interval correlator will give an output pulse for every symbol when the data symbol has the same FFT length as the P1 symbol. Therefore, some different mechanism must be applied to distinguish the P1 symbol with the data symbols if both of them have same FFT length.

In the presence of CW interferers, a complex DC component is superimposed on the output of the guard interval correlator, whose amplitude and phase depends on the corresponding amplitude and frequency offset of the interferer. This problem can be solved by using a high pass filter but it will add some more delay because of the settling time needed by this filter. Lastly, if delayed path is present in the propagation channel in addition to the first path like SFN implementation, then dangerous delay values will be generated that will cause some problems. For instance, if the propagation channel has a second path delayed by duration T_A with respect to the first one, then there will be a perfect correlation between the direct-path component at the output of the correlator delay element and the delayed-path component at the input to the correlator delay element. Therefore a noisy DC offset will be present at the correlator output.

The A-B structure can easily determine the fractional part of the frequency offset by noting the argument of the complex correlation pulse generated by the receiver processing chain. This argument increases by 2π radians for every increase of frequency offset equal to the OFDM-symbol carrier spacing. However, this carrier spacing is the reciprocal of T_A and therefore $f_{OFFSET}\ T_A$ will provide the offset in units of carrier spacings. As mentioned previously, this frequency offset has one integer part and one fractional part. The fractional part can be calculated according to the following formula:

$$Fractional\ part\ of\ (f_{OFFSET}\ T_A) = \frac{arg(pulse)}{2p} \qquad (5.1)$$

5.3.1.2.2 A-B structure with frequency shift

The problems in simple A-B structure motivated to include only one modification in the P1 symbol. This modification is implemented by employing frequency shift in part B, keeping all others as same as the previous one. This modified structure with frequency shift applied to part B is presented in Figure 5.4.

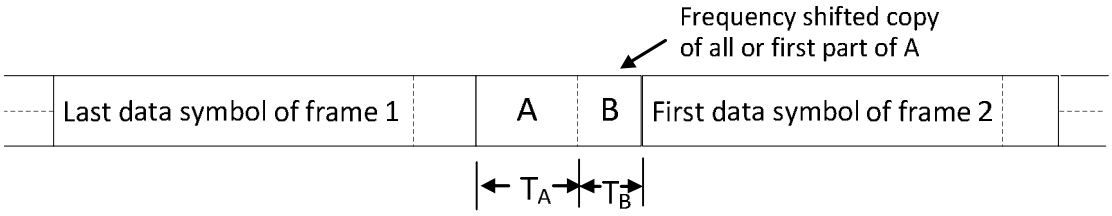

Figure 5.4. *P1 symbol, A-B structure with frequency shift.*

The receiver processing chain for this modified structure can be derived from the previous receiver chain and is presented in Figure 5.5 [40]. Here the frequency shift is denoted by f_{SH}, and so part B is simply multiplied by $exp(j2\pi f_{SH}t)$ to implement the frequency shifting.

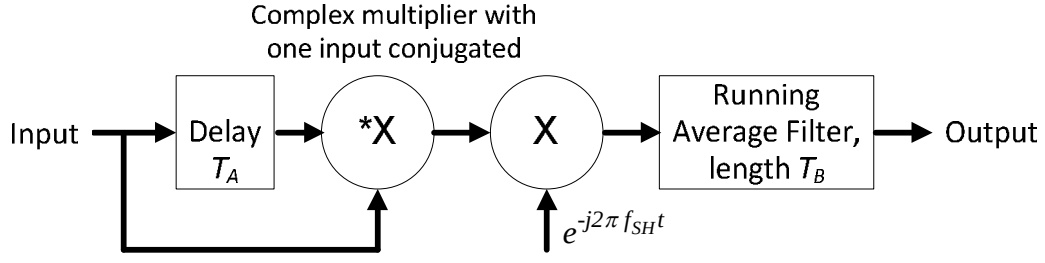

Figure 5.5. *Receiver processing chain for A-B structure with frequency shift.*

This frequency shift can be chosen as the whole number of P1 symbol carrier spacings to make the implementation simpler. If the conjugation is applied to the delayed component, then the multiplier output will have an upward shift by f_{SH}, because of the frequency shifting in the structure. Therefore, multiplying the multiplier output by $exp(-j2\pi f_{SH}t)$ is enough to downshift it.

It is found that the A-B structure with frequency shift in part B is quite useful as it solves the problems of false detections, CW interferers and dangerous delays encountered with the previous structure. In this case, only the P1 symbol has the frequency shift, while the data symbols do not have. So if a data symbol having the same FFT length as P1 symbol is passed through this processing chain, then the first multiplier will result in an unshifted correlation, which will be downshifted by f_{SH} by the second multiplier. If the length of the running average filter has a whole number of cycles of f_{SH}, then this filter will be able to cancel the false unwanted pulse.

Moreover, the impact of the CW interferers that used to produce a complex DC constant value at the output of the first conjugated multiplier, will now produce a complex exponential $exp(-j2\pi f_{SH}t)$. This will be averaged out by the running average filter when the length of this filter has a whole number of cycles of the frequency shift. Furthermore, this modified structure will get rid of dangerous delay values produced by the existence of a second path component delayed by T_A with respect to first path, which used to cause an unwanted noisy DC offset at the correlator output.

Although the frequency shift in this modified A-B shifted structure helps to solve some problems of the previous A-B structure, but it has a significant drawback. By using this A-B shifted structure, it will be difficult to determine the fractional part of the frequency offset, which was easily possible by A-B structure by noting the argument of the complex correlation pulse.

If any frequency offset is present in the input of the receiver processing chain, then it affects the argument of the correlation peak by adding another angle. This angle is related to the arbitrary phase of the oscillator of the receiver as compared with the phase of the shifted waveform at the transmitter, together with the effect of the path delay. This argument increases by 2π radians for every increase of frequency offset equal to OFDM symbol carrier spacing. Therefore it will be difficult to deduce the fractional part of the frequency offset by noting the correlation peak argument because of the unknown angle added to the angle caused by the frequency offset.

5.3.1.2.3 C-A-B structure

Further modification is needed for the proposed P1 symbol in order to solve all the problems of the previous two proposals. Therefore a different structure is proposed that has another frequency shifted part added in the beginning of the previous structure. Thus the P1 symbol will have a frequency shifted part C, followed by the original complete FFT symbol part A, and another frequency shifted part B, shown in Figure 5.6. Here part C will have the same length and frequency shift as part B and both of them essentially are the frequency shifted copy of all or first part of A.

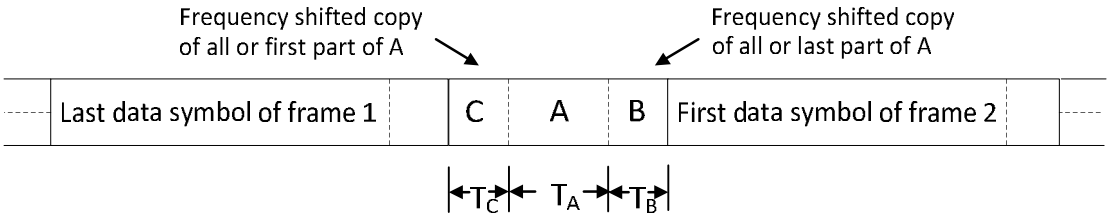

Figure 5.6. *P1 symbol, C-A-B structure.*

The receiver processing chain corresponding to this structure is given in Figure 5.7, where the guard interval correlator output is divided into two frequency-shifter and running average filter combinations. The shifter in upper combination shifts up in frequency, hence detects the correlation between C and A. On the other hand, the shifter in lower combination shifts down in frequency, thus detects the correlation between A and B. The shifter-filter outputs are multiplied after the upper filter output is delayed by T_B, because the correlation between A and B occurs T_B later than that between C and A.

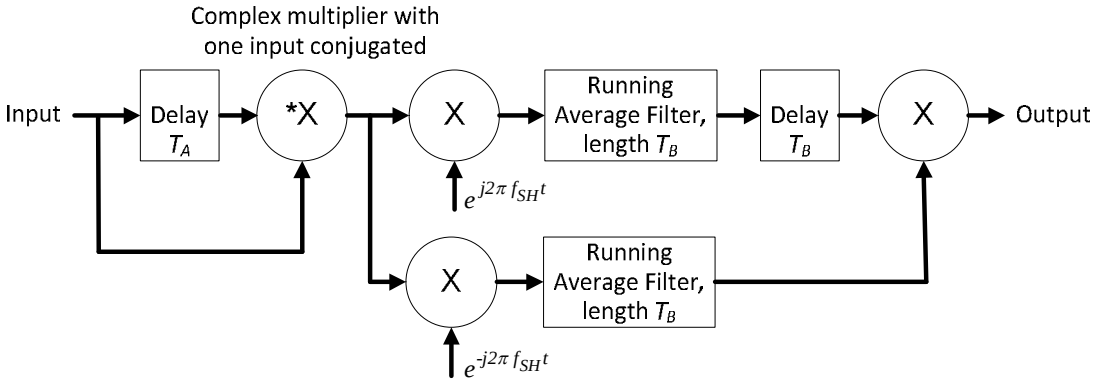

Figure 5.7. *Receiver processing chain for C-A-B structure.*

This structure overcomes the disadvantages of the previous two P1 symbol structures. Now the fractional part of the frequency offset can be obtained from the argument of the output pulse and the problems of false detection, CW interferers and dangerous delays are also solved. However, the only less significant disadvantages of this structure are that the length of the P1 symbol is increased to accommodate part C and correspondingly the complexity of detecting the P1 symbol is also slightly increased.

The C-A-B structure is able to determine the fractional part of the frequency offset by noting the argument of the correlation peak just like the A-B structure and thus solves the problem encountered by A-B shifted structure. In the receiver processing chain for C-A-B structure, the two running average filters are affected by an unknown rotation that results from the arbitrary shift of the oscillator of the receiver.

However, the same receiver oscillator is used for both branches but in opposite shift directions, so the two rotations will be in opposite directions. The unknown rotation can be cancelled by multiplying the outputs of these two running average filters. Therefore the actual rotation caused by the frequency offset at the receiver acts in the same direction for both branches and the argument of the correlation peak becomes double than that given in Equation (5.1). Hence it is possible to deduce the fractional part of the frequency offset by this C-A-B structure.

5.3.1.3 P1 symbol generation

The actual P1 symbol structure in DVB-T2 standard was inspired by the C-A-B structure described in the last subsection, and was implemented with few modifications both in the symbol structure and in the receiver processing chain. The following subsections present the symbol structure, carrier distribution, modulation and time domain signal generation for P1 symbol [4].

5.3.1.3.1 P1 symbol structure

The structure and length of P1 is fixed and does not depend on the FFT mode or guard interval size of the OFDM data symbols. The purpose of fixing this is to make the detection task easier for the receiver as it will always look for the symbol which has fixed length and structure. In addition, P1 symbol has such a structure that makes it possible to detect this symbol in the presence of significant frequency offset [4]. Figure 5.8 presents the structure of the P1 symbol.

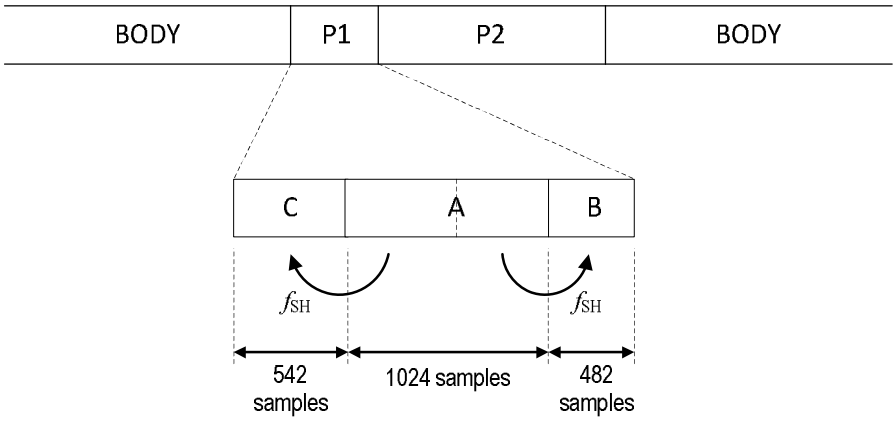

Figure 5.8. *P1 symbol structure [4].*

P1 symbol contains frequency shifted repetitions of the main part of itself and it has a structure that has three parts: part C, A and B. The main part of P1 symbol is the part A, which is a 1K OFDM symbol. Part C is the frequency shifted copy of the first 542 samples of part A and part B is the frequency shifted copy of the last 482 samples of part A. Actually, a 1K symbol can be transmitted by 853 useful carriers within the nominal bandwidth. However, 766 carriers from the middle are considered only and among them, 384 carriers are used as pilots, while other carriers are set to zero. The first active carrier starts from carrier 44 and the last one finishes at carrier 809. Figure 5.9 shows the active carriers of P1 symbol and their positions.

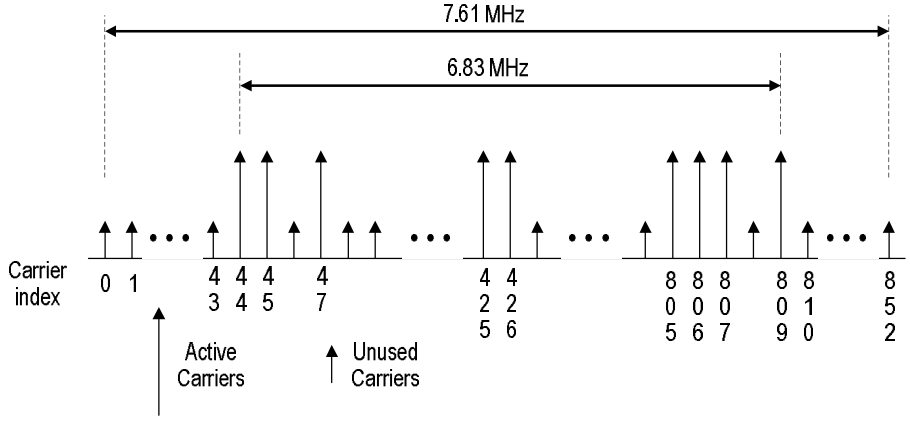

Figure 5.9. *Active carriers of the P1 symbol [4].*

The active carriers are centered in the middle occupying roughly 6.83 MHz band from the middle of the nominal 7.61 MHz signal bandwidth for the 8 MHz

system. This design enables the receiver to tolerate a maximum frequency offset of 500 KHz because most of the used carriers will still be within the 7.61 MHz nominal bandwidth. As a result, the symbol can be recovered by tuning the receiver to the nominal centre frequency [4].

The block diagram of P1 symbol generation is given in Figure 5.10. The tasks carried out in the block diagram are discussed in the following subsections.

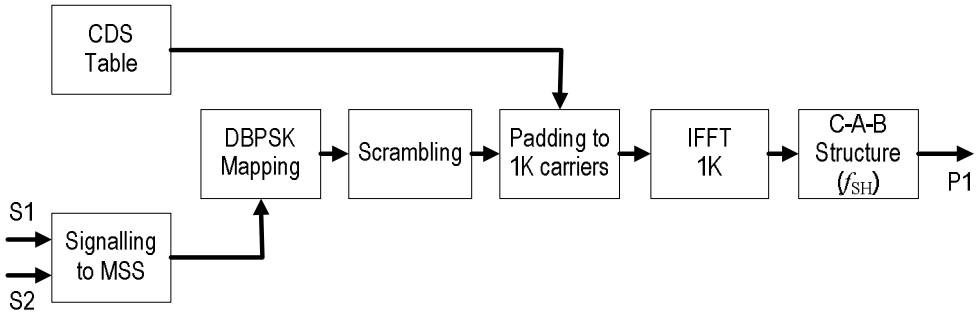

Figure 5.10. *Block diagram of P1 symbol generation [4].*

5.3.1.3.2 Carrier distribution

Carrier distribution in P1 symbol is done by using three complementary sequences. The first and the last sequences are 128 chips long, while the middle sequence is 512 chips long. The last two zero bits of the third sequence makes the total number of carriers to 766. These three sequences have 64, 128 and 64 values respectively for active carrier positions, thus resulting in 384 active carriers among those 766 carriers. The Carrier Distribution Sequence (CDS) table (Figure 5.10) can be found in DVB-T2 standard [4].

5.3.1.3.3 Modulation

Active carriers are Differential Binary Phase Shift Keying (DBPSK) modulated with a modulation pattern for encoding two signalling fields, known as S1 and S2. P1 symbol has the capability to convey 7 bits. Among them, S1 field can encode 3 bits and thus can signal 8 values. However, S2 field can signal 16 values by encoding 4 bits. Moreover, patterns to encode S1 field have 8 complementary hexadecimal sequences, each of length 16 that will result in a binary sequence of length 64. On the other hand, patterns to encode S2 field have 16 hexadecimal sequences, each of length 64, resulting in a binary sequence of length 256.

P1 symbol carries two types of information: the first one is carried by S1 field to distinguish the preamble format and frame type and the second one is carried by S2 field to signal FFT size to the receiver, as presented in Table 5.1, Table 5.2 and Table 5.3 respectively [4].

S1 field	Preamble format/ P2 Type	Description
000	*T2_SISO*	The preamble is a T2 preamble and the P2 part is transmitted in its SISO format
001	*T2_MISO*	The preamble is a T2 preamble and the P2 part is transmitted in its MISO format
010, 011, 100, 101, 110, 111	*Reserved*	Reserved for future systems, including a system having both T2-frames and FEF

Table 5.1. *S1 field of P1 symbol.*

S1 field	S2 field	FFT size	Description
00X	000X	2k	Indicates the FFT size of the symbol in the T2 frame
00X	001X	8k	
00X	010X	4k	
00X	011X	1k	
00X	100X	16k	
00X	101X	32k	
00X	110X	Reserved for future	-
00X	111X	Reserved for future	-

Table 5.2. *S2 field for P1 symbol, complementary information.*

S1 field	S2 field	Meaning	Description
XXX	XXX0	Mixed	All preambles in the current transmission are of the same type as this preamble
XXX	XXX1	Not mixed	Preambles of different types are transmitted

Table 5.3. *S2 field for P1 symbol, mixed bit information.*

The patterns to encode S1 and S2 have two main properties. Firstly, the sum of the auto-correlations of all the sequences of the set is equal to a Krönecker delta, multiplied by KN factor, where K is the number of the sequences of each set and N is the length of each sequence. For S1, K=N=8; and for S2, K=N=16. Secondly, each set of sequences are mutually uncorrelated. The S1 and S2 modulation patterns are given in DVB-T2 standard [4].

In order to obtain the modulated signal, the following tasks are performed sequentially. At first, the S1 and S2 sequence are concatenated and the S1 sequence is again added at the end. This sequence then is modulated by DBPSK. The modulated sequence then goes through bit-by-bit scrambling by the 384 bit scrambler sequence. After that, the scrambled sequence is mapped to the active carriers with a boosting to ensure that the power of P1 symbol is virtually same as the power of the remaining symbols. The boosting amount is a voltage ratio of root of (853/384) or 3.47 dB, because P1 symbol uses only 384 active carriers out of 853 carriers available for a 1K OFDM symbol. Later on, appropriate padding is added to map the 384 carriers into 1K carriers.

5.3.1.3.4 Time domain signal generation

In the beginning, the useful part, i.e., part A is generated from the carrier modulation sequence by the following equation

$$p_{1A}(t) = \frac{1}{\sqrt{384}} \sum_{i=0}^{383} MOD\_SCR_i \times e^{j2\pi \frac{k_{P1}(i)-426}{1024\,T} t} \qquad (5.2)$$

where $k_{P1}(i)$for i=0,1,…,383 are the indices of the 384 active carriers, MOD_SCR_i for i=0,1,…,383 are the modulation values for the active carriers and T is the elementary time period.

After generating the useful part, denoted by P1(A), two frequency shifted guard intervals are added with it to improve the robustness of P1 symbol. Therefore, the first guard interval part C, denoted by P1(C), is added before P1(A) that contains first 542 frequency shifted samples of P1(A). In the same way, the last guard interval part B, denoted by P1(B), is added after P1(A) that contains last 482 frequency shifted sample of P1(A). The applied frequency shift f_{SH} is given as 1/1024T. The time domain baseband waveform $P_1(t)$ of P1 symbol is given according to given equation:

$$P_1(t) = \begin{cases} P_{1A}(t)\, e^{j\frac{2\pi}{1024\,T}t} & ,0 \le t < 542T \\ P_{1A}(t - 542T) & ,542T \le t < 1566T \\ P_{1A}(t - 1024T)\, e^{j\frac{2\pi}{1024\,T}t} & ,1566 \le t < 2048T \\ 0 & ,otherwise \end{cases} \qquad (5.3)$$

5.3.1.4 P1 symbol detection

The P1 detection can be achieved by correlating the two guard interval portions added in both sides of the useful 1K OFDM symbol. The correlation will be based on two branches running in parallel, where each branch will be looking for the maximum similarity of the respective part of the repetition [19]. The implementation given in Figure 5.11 performs the correlation for both guard interval parts of the P1 symbol and the correlations will give their maximum peaks in the presence of P1 that indicates the detection of P1 symbol.

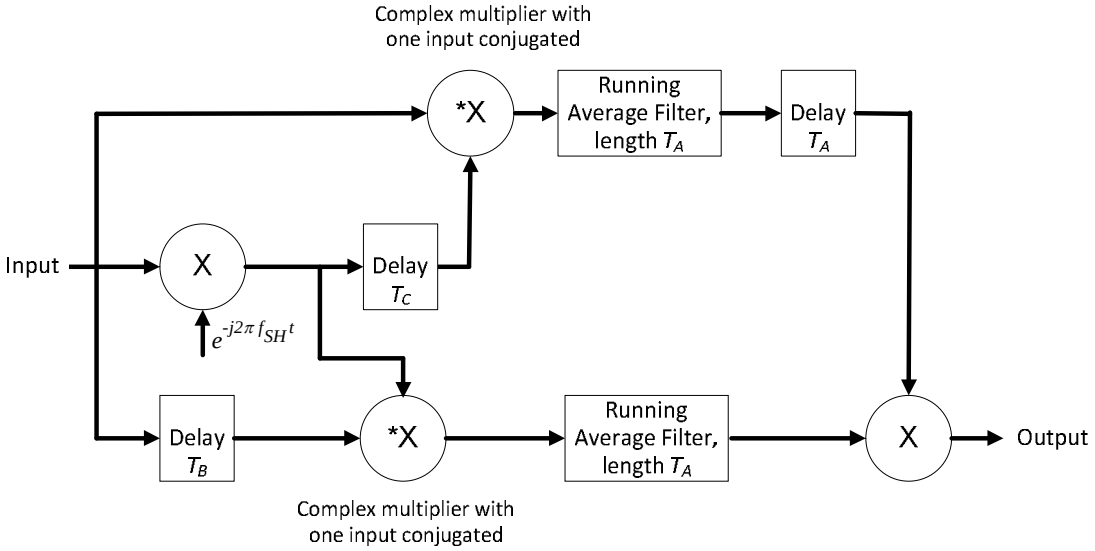

Figure 5.11. *Correlation chain block diagram for the P1 detection [19].*

The frequency shift is represented by f_{SH} and T_A, T_B and T_C correspond to 1024, 482 and 542 samples respectively to parts A, B and C of the P1 symbol. The delay elements T_C and $T_{B,}$ together with an associated multiplier and running-average filter of length equal to reciprocal of f_{SH} forms a correlator type circuit in order to detect the frequency-shifted repetition in the signal in parts C and B respectively. However, the other delay element T_A ensures that the outputs of these two correlators are aligned in time domain.

The structure in Figure 5.11 generates two correlator outputs of complex pulses, whose magnitude is a trapezoidal pulse that has a base of duration $(T_A + T_X)$, sloping sides of duration T_X, and top of duration $(T_A – T_X)$, where T_X takes the value T_C or T_B respectively for the two correlators. The two correlator output pulses are multiplied to cancel the effect of the unknown arbitrary phase of the down-shifter

oscillator. Therefore, the argument of the final output pulse can be shown to be proportional to the fine or fractional component of the frequency offset.

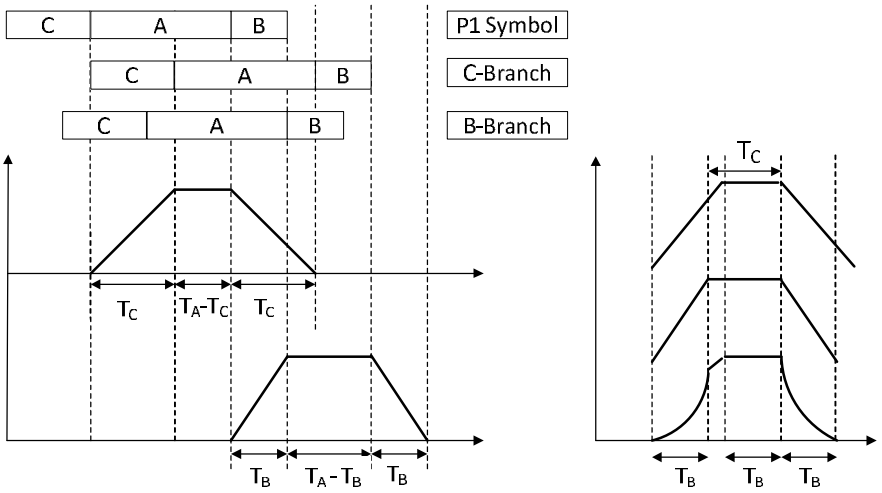

Figure 5.12. *Correlation peak for the P1 detection [19].*

The outputs of the correlators are given in Figure 5.12, where the left figure shows the outputs of the two correlations, and the right figure shows the time-alignment and multiplication of them. The timing of this pulse can be used to select the 1024 samples long useful A part of the P1 symbol. As a result, FFT window position can be determined and demodulation can be performed. The presence of P1 can be detected by applying a suitable threshold to the magnitude of the correlator output, and thus can conclude the presence of a DVB-T2 signal [19].

5.3.1.5 P1 symbol validation

The goal of P1 validation is to confirm the correct reception of the P1 symbol, meaning that, whether the incoming symbol matches with the distribution of the carriers specified for the P1 symbol. Though the distribution is received as expected, but it can be found in different locations shifted from their original locations. Therefore, this step also reports and corrects the coarse or integer component of the carrier frequency offset. The P1 validation can be achieved by correlating the distribution across the carriers of the received P1 symbol with the expected CDS [19].

The active carriers in P1 symbol are distributed keeping a safety area padded by zero at both ends. It makes the detection of the correlation peak possible even if the frequency of the transmitted signal is inside ±500 kHz range from the centre of the

bandwidth for 8 MHz systems. Moreover, the peak of the correlation will report the integer number of carriers that the symbol is shifted, which corresponds to the coarse frequency offset.

5.3.1.6 P1 symbol decoding

At this stage, the P1 structure is assumed to be correctly detected and the system knows which of the active carriers are used. Then the received P1 sequence has to be extracted from the carrier distribution and unscrambling and de-mapping has to be performed in order to decode the P1 signalling. In the transmitter, the signalling field S1 and S2 are encoded with specified patterns. Therefore, those signalling fields can be obtained in the receiver by performing a simple comparison between the received sequences with those expected patterns [19].

Decoding the P1 symbol will provide the basic transmission parameters. At first, P1 symbol will disclose the fact that whether it belongs to a T2 frame or to a FEF part, because it is possible to find the FEF parts within the same channel carrying the T2 signal. Then decoding the P1 symbol will give the FFT size and SISO or MISO mode of transmission.

5.3.2 Synchronization using pilots and P2 symbol

The P1-symbol detection and decoding process can give a fast estimate of the FFT window position and the carrier frequency offset. However, there might be some error in both these estimates. Moreover, P1 signal cannot be used to estimate the sampling-frequency error.

In this situation, it is expected that the receiver will use one of the many existing synchronization algorithms to perform fine synchronization in time and determine coarse frequency offset. DVB-T2 frame structure has subcarriers reserved for carrying known pilots that are multiplexed with data in the frequency domain and thus can be interpreted as superimposed to the time domain signal. The synchronization algorithms typically use the continual pilots for estimating error in frequency, together with an impulse response estimate derived from the scattered pilots for fine adjustment of the FFT window position [19]. Since DVB-T2 has both the continual and scattered pilots just like DVB-T, so the synchronization methods of DVB-T can be used in DVB-T2 after making necessary adaptation. The idea of using pilots prior to the reception FFT operation has been discussed first by Wang et al.

[41], its exploitation has been extended to the refinement of time synchronization by Filippi et al. [42], and full synchronization method has been discussed by Jahan et al. [39].

The synchronization methods in DVB-T2 use algorithm in order to achieve all form of synchronizations, such as sampling-clock, symbol, frequency and frame synchronization. This algorithm uses all types of pilots, especially scattered pilots to provide a robust synchronization that does not depend on the channel. DVB-T2 can achieve synchronization even at SNRs below -6dB to -12dB, which depends on the used FFT size and pilot pattern type. The algorithm uses scattered pilots to perform the cross-correlation between the received signal and the time representation of the scattered pilot sequence. After that, the complex correlation results are successively exploited to achieve sampling-clock and symbol synchronization at first, then frequency synchronization and finally frame synchronization [19].

However, the receiver needs to know the scattered pilot pattern used during the transmission for applying the algorithms that exploits the scattered pilots. Therefore, the receiver needs to decode the P2 symbol in order to know the scattered pilots pattern in the data symbols. In addition, P2 symbol also conveys other information, like the use of extended or normal carrier mode, PAPR technique, frame length, L1 signalling length etc. When P1 symbol has been recovered and basic transmission parameters are known by decoding it, after that P2 symbol is decoded in order to extract the necessary information [19].

6. Simulation and Results

Previous chapters have explained the theoretical background for synchronization in DVB-T2. This chapter concentrates on providing information about the simulation performance and results. The first section of this chapter discusses the tuning of the simulation model. Then the next section presents the performance analysis for P1 symbol evolution. Finally, the performance of this P1 symbol has been analyzed in the presence of AWGN, static Rayleigh, static SFN and dynamic TU6 channels.

6.1. Simulation model tuning

Before running the simulation to analyze the performance of P1 symbol, the simulation model is needed to be tuned in order to work perfectly. The first task of this simulation model is to detect the presence of the P1 symbol and a threshold is used for this purpose. When the correlator output pulse crosses the threshold, then it can be concluded that the P1 symbol is present in the corresponding channel. Therefore the system carries out the synchronization and decoding tasks after detecting the P1 symbol in the channel. This implies the importance of choosing an appropriate threshold. If the threshold is not chosen carefully, then it will lead to incorrect detection and the rest of the tasks of the simulation model will also be incorrect.

Probability of detection measures the probability of detecting the P1 symbol in the transmission channel. On the other hand, probability of false detection measures the probability of detection when a data symbol is sent instead of the P1 symbol. The threshold for detection is chosen based on the correlation peak produced by the receiver processing correlation chain. It is chosen in such a way that the probability of

detection will be increased, but at the same time the probability of false detection will be decreased for a given SNR value.

If the threshold is chosen to be high enough, then the probability of detection will be low at very high SNR, which is not desirable. However, this situation will keep the false detection probability at a very low value, which is good. On the other hand, if the threshold is chosen to be low enough, then there might be a high probability of false detection at very low SNR. Though this low threshold value will maximize the detection probability, but it is also not desirable because it will increase the false detection probability.

The synchronization tasks are also dependent on the output of the receiver processing chain correlator output. Firstly, the coarse timing synchronization is done by noting the index of the peak of the correlator output as it gives the starting point of the T2-frame. Moreover, the argument of the complex valued correlator peak provides an estimate of the fractional component of the frequency offset. Therefore, detecting the peak of the correlator output is very important for achieving the coarse timing synchronization and determining fractional frequency offset.

6.2. P1 symbol evolution simulation results

The evolution of the P1 symbol structure and corresponding receiver processing chain for these structures during the development phase has been discussed in section 5.3.1.2. Hence, this subsection provides simulation results for all these structures in order to show the capabilities and drawbacks of each and describes the need for the next structure.

6.2.1 A-B structure

According to the first proposal for P1 symbol, a single unique signal discovery symbol with different characteristics than the data symbol is to be inserted in the beginning of every T2-frame. This P1 symbol has one useful part, called part A, and another guard interval part, called part B (Figure 5.2). Two T2-frames are considered for simulation and each one of them starts with a P1 symbol. However, the observation window is considered such that it includes the data symbols of the first frame, then the P1 symbol and data symbols of the second frame.

A DVB-T2 system has been developed in Matlab for simulation. Then corresponding receiver processing chain for A-B structure (Figure 5.3) has been produced to analyze the effect of the P1 symbol. The channel is AWGN channel unless otherwise specified. The common parameters used in the simulation are given in Table 6.1.

Parameter	Value	Symbol
FFT-length of the data symbols	2048	N
Guard Interval of the data symbols	512	GI
Number of data symbols in each T2-frame	4	-
Modulation in the data symbols	16-QAM	-

Table 6.1. *Parameters for T2-frame.*

The initial idea for P1 symbol before standardization was to insert a unique symbol in the transmitter and later detect it in the receiver. However, the FFT-length and the duration of the guard interval part of P1 symbol were not fixed. DVB-T2 supports many different FFT-lengths and guard intervals for its data symbols. Therefore, it might happen that the data symbols and the P1 symbol have the same FFT length and guard interval duration. The useful duration of P1 symbol is represented by T_A and the guard interval part is represented by T_B.

For the simulation, at first the P1 symbol has been designed such that the main useful part A has FFT-length of 1K and has been modulated by 16-QAM. So the data symbols and P1 symbol have different FFT-lengths, but they have the same modulation. As part B of the P1 symbol can be a copy of all or first part of A, hence part B has been chosen as a complete copy of A. So the P1 symbol has 100% guard interval duration.

Now the next step would be to detect the presence of P1 symbol by the receiver processing chain and to determine the starting position of the T2-frame. The system model has been simulated in almost noise-free AWGN channel with 200 dB SNR. The correlator output has been presented in Figure 6.1. If the receiver is able to detect a correlation peak like this figure, then correspondingly it can be sure about the presence of P1 symbol in the channel.

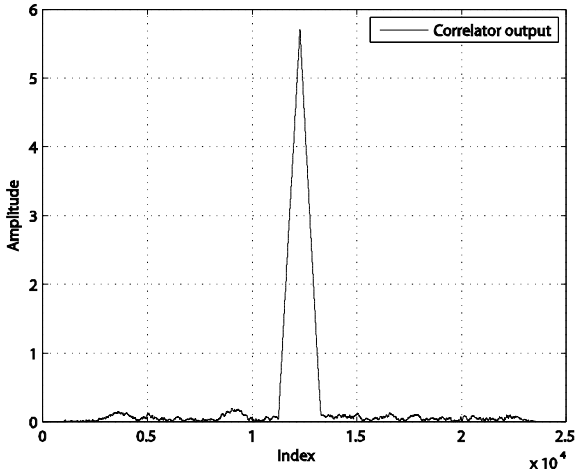

Figure 6.1. *Correlator output of the receiver processing chain for A-B structure.*

As mentioned earlier, the peak position of the correlator output provides the starting position of the T2-frame. The Mean Squared Error (MSE) value for a range of SNR values for timing synchronization is given in Figure 6.2(a). In addition, the argument of the complex valued peak provides the fractional component of the frequency offset. Figure 6.2(b) presents the MSE vs. SNR curve for estimating the fractional frequency offset. The amount of initial frequency offset that has been introduced in all frequency offset estimation was 0.12.

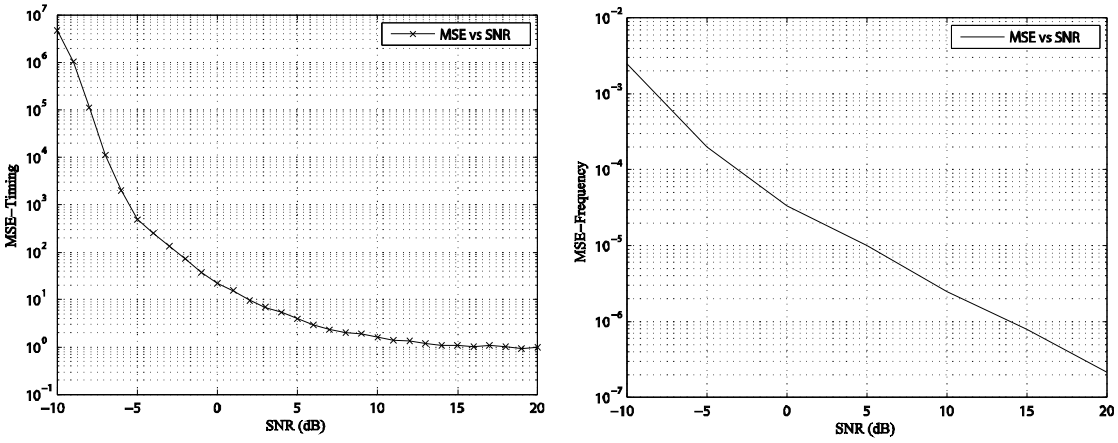

(a) (b)

Figure 6.2. *(a) MSE-Timing vs. SNR (b) MSE-Frequency vs. SNR.*

However, this structure has some problems of false detection, and in the presence of Continuous Wave (CW) interferers and dangerous delays, as mentioned in section 5.3.1.2. The false detection problem states that whenever the data symbol and the P1 symbol has the same FFT-length, then the corresponding receiver processing

chain will give a pulse at each of the data symbol and for the P1 symbol. Hence the detection of the P1 symbol will be problematic in this scenario.

False detection occurs when the guard interval of the data symbol and the B part of the P1 symbol has the same length, in addition to their similar FFT-length. To test this, we have kept all the settings of the previous system but changed the guard interval part B of the P1 symbol to be same as the guard interval of data symbols, meaning that, $T_A = N$ and $T_B = GI$. The simulation result is presented in Figure 6.3(a) and we can see the false detection pulses for every data symbols and for the P1 symbol. Hence the receiver is no longer able to differentiate the P1 symbol with the data symbol by analyzing the output of the receiver processing chain. The MSE for timing synchronization given in Figure 6.3(b) proves that the timing synchronization fails for this parameter setting.

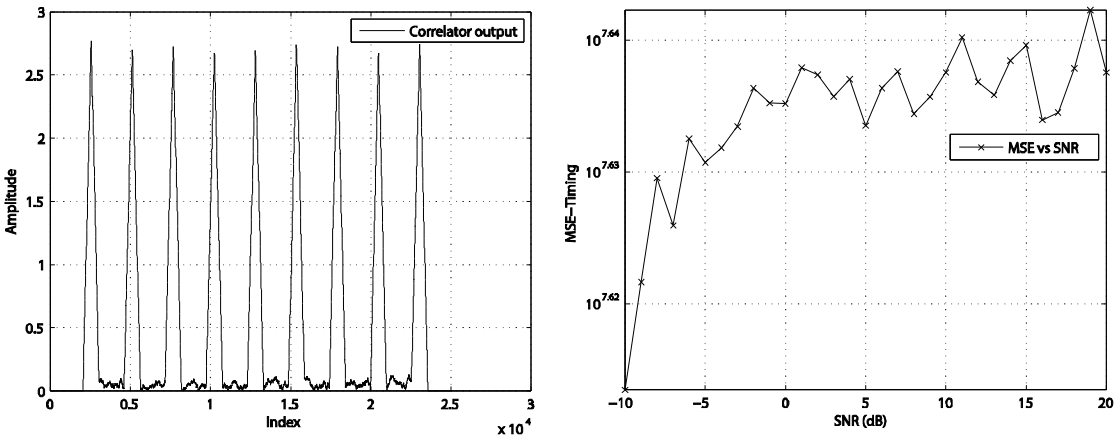

(a) (b)

Figure 6.3. *(a) Correlator output for $T_A = N$ and $T_B = GI$ (b)MSE-Timing vs. SNR.*

The A-B structure also suffers when the received signal contains CW interferers as it causes a complex DC constant value to be superimposed at the output correlation peak of the receiver processing chain. The amplitude and phase of this DC component depends on the amplitude and frequency offset of the interferer. In the simulation, the amplitude of the CW interference has been chosen as unity to have the same power of data symbols. The amount of CW shift has been chosen as *0.3*. In frequency, it is around 1 KHz. Figure 6.4(a) presents the output of the receiver processing chain when $T_A = N$ and $T_B = T_A$ and Figure 6.4(b) represents the output when $T_A = N$ and $T_B = GI$. It can be clearly observed that the single correlation peak is superimposed by the DC-component.

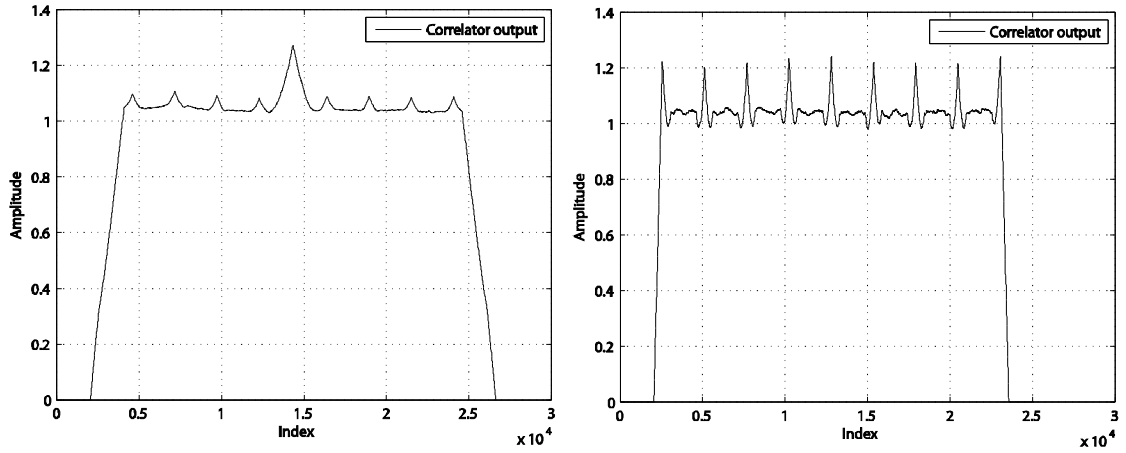

(a) (b)

Figure 6.4. *Correlator output for CW interferer (a)T_A=N & T_B=T_A (b)T_A=N & T_B=GI.*

Furthermore, A-B structure shows inconsistency in SFN channels where a delayed path is present in addition to the first path. This problem is referred as dangerous delays problem. For simulation, SFN channel is created by using two static Rayleigh channels with a delay equals to T_A present between the two paths of the channel model. If the relative delay between the first and the second path is equal to the duration of the useful part A of the P1 symbol (T_A), then the output of the receiver processing chain contains a noisy DC offset.

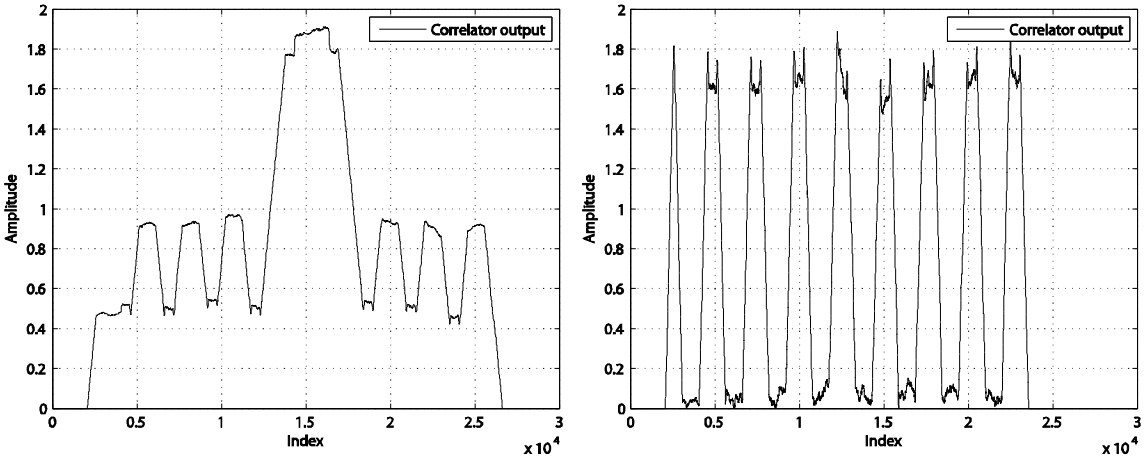

(a) (b)

Figure 6.5. *Correlator output for SFN channel (a) T_A=N & T_B=T_A (b)T_A=N & T_B=GI.*

The output of the receiver processing chain for $T_A = N$ and $T_B = T_A$ is presented in Figure 6.5(a). In this figure, the triangular correlation peak is distorted by the noisy DC offset and the presence of side-lobes will make the detection difficult in severe channel condition. Moreover, the correlator output for $T_A = N$ and $T_B = GI$ is presented

in Figure 6.5(b) where it is practically impossible to distinguish the presence of the correlation peak for the P1 symbol.

6.2.2 A-B structure with frequency shift

The modified A-B structure of P1 symbol with frequency shift has only one difference with the previous A-B structure. Now the guard interval part B of P1 symbol has been frequency shifted (Figure 5.4) and the receiver processing chain has been modified accordingly (Figure 5.5). Therefore the running average filter will be able to cancel the false unwanted pulses of the side-lobes if the length of this filter has a whole number of cycles of the frequency shift. The value of the integer number of cycles of the frequency shift has been chosen as unity for the simulation results presented in this subsection.

This A-B structure with frequency shift in part B is able to overcome the problems of false detections, CW interferers and dangerous delays that were associated with the previous A-B structure. In order to show that the A-B shifted structure does not have the false detection problem, we keep the worst case scenario where the previous A-B structure was giving false detection pulses. Hence, the useful part of P1 symbol has the same FFT-length as the data symbol and guard interval part B has the same duration as the guard interval of the data symbols, meaning that, $T_A = N$ and $T_B = GI$. The output of the receiver processing chain is presented in Figure 6.6(a). We can observe that the false detection correlation peaks for the data symbols are no longer present. Thus A-B shifted structure solves the false detection problem. The MSE-Timing vs. SNR for this configuration is also given in Figure 6.6(b).

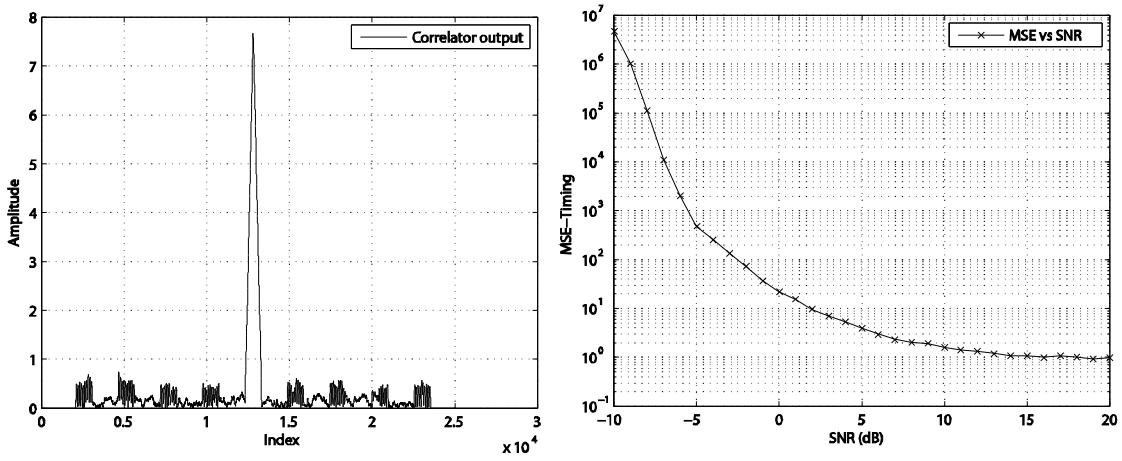

(a) (b)

Figure 6.6. *(a) Correlator output of receiver processing chain for A-B structure with frequency shift to solve false detection problem (b) MSE-Timing vs. SNR.*

The A-B shifted structure also eliminates the problem of CW interferers. The complex DC constant value that appears at the output of the first conjugated multiplier of the receiver processing chain (Figure 5.5), has been converted to a complex exponential. This complex exponential is exactly averaged out by the running average filter if the frequency shift and the running average filter are related, as already discussed above for false detection case.

Figure 6.7(a) presents the output of the receiver processing chain for A-B shifted structure when $T_A = N$ and $T_B = T_A$ and Figure 6.7(b) represents the output when $T_A = N$ and $T_B = GI$. In both these simulation results, the single correlation peak is clearly detectable, which were not possible for the simulation results of A-B structure (Figure 6.4). Thus the frequency shift in the part B allows the A-B shifted structure to overcome the CW interference problem.

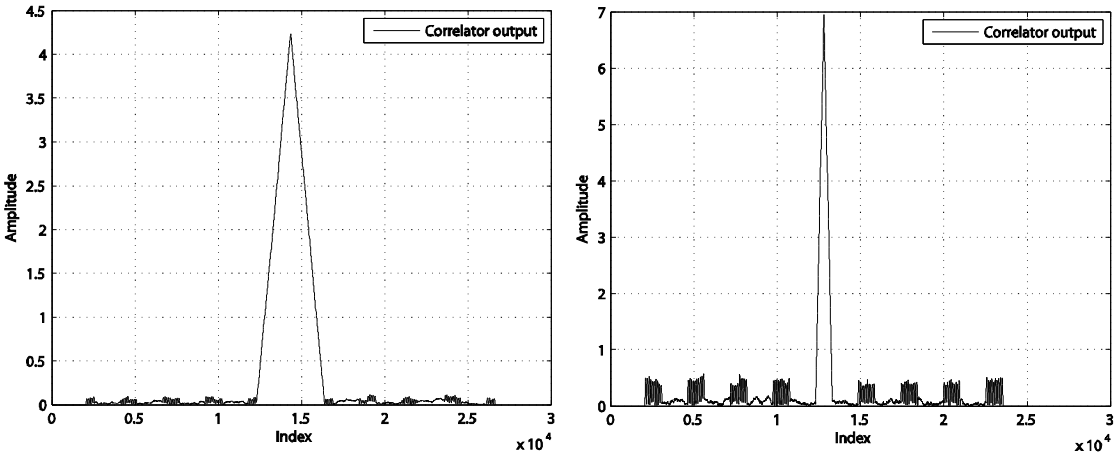

(a) (b)

Figure 6.7. *Correlator output for CW interferer (a)T_A=N & T_B=T_A (b)T_A=N & T_B=GI.*

The unwanted effects of dangerous delays are also possible to overcome in this A-B shifted structure by maintaining the relation of frequency shift and the length of the running average filter discussed in the above two cases. The simulation results keeping the same conditions as the simulation for A-B structure for dangerous delays are presented in Figure 6.8.

The output of the receiver processing chain when $T_A = N$ and $T_B = T_A$ is presented in Figure 6.8(a) where we can observe that the side-lobes are suppressed. Though the correlation peak is not a single triangular one, but it is nevertheless possible to detect the presence of P1 symbol. Moreover, the output when $T_A = N$ and $T_B = GI$ is presented in Figure 6.8(b) where two correlation peaks are present instead

of one for the P1 symbol. However, it is still possible to detect the presence of the correlation peak by setting an appropriate threshold

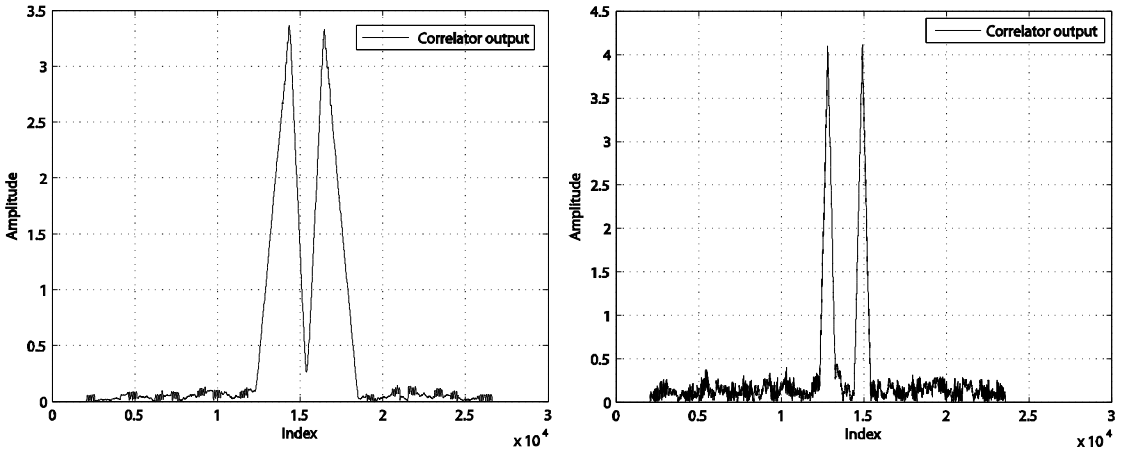

(a) (b)

Figure 6.8. *Correlator output for SFN channel (a) T_A=N & T_B=T_A (b)T_A=N & T_B=GI.*

However, the A-B structure with frequency shift in part B has one problem. This structure does not provide accurate estimate of the fractional part of the frequency offset, which was previously possible for A-B structure by noting the argument of the complex correlation peak of the receiver processing chain. For the A-B structure with frequency shift, one unknown angle is added to the argument of the correlation peak if any frequency offset is present in the input of the receiver processing chain. This angle is related to the arbitrary phase of the receiver oscillator as compared with the phase of the shifted waveform at the transmitter, combined with the effect of the path delay. Hence it will be difficult to determine the fractional part of the frequency offset.

The A-B structure with frequency shift has been simulated in the presence of constant frequency offset at the transmitter. Correspondingly, MSE for estimating fractional frequency offset for different SNR values has been calculated in the receiver. The channels that have been used are Rayleigh and SFN channels. Figure 6.9(a) presents the MSE-Frequency vs. SNR for Rayleigh channel and Figure 6.9(b) presents for SFN channel. Two static Rayleigh channels are used as the two paths for the SFN channel with a delay of T_A present between the paths. From the figures, it can be seen that the Frequency offset estimation has larger MSE value even at higher SNR. The reason is this argument increases by 2π radians for every increase of frequency offset equal to OFDM symbol carrier spacing. Therefore it will be difficult

to deduce the fractional part of the frequency offset by noting the argument of the complex correlation peak.

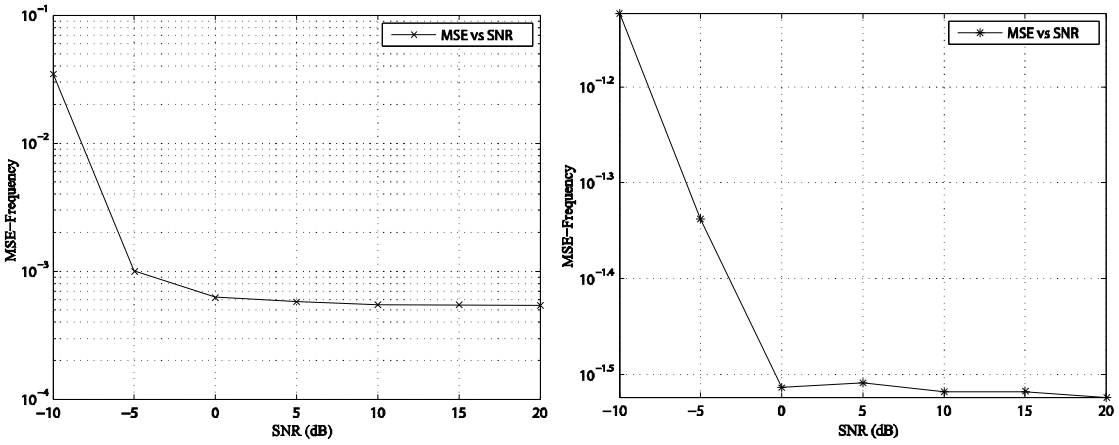

(a) (b)

Figure 6.9. *MSE-Frequency vs. SNR for constant frequency offset estimation (a) Rayleigh channel (b) SFN channel.*

6.2.3 C-A-B structure

The structure for P1 symbol has been modified further by adding another frequency shifted part in the beginning of the previous structure. In C-A-B structure, another part, named part C, is inserted before part A and part B. Both part C and part B are of same length and have the frequency shifted copy of all or first part of A (Figure 5.6). Therefore this structure has two frequency shifted parts of same length and the frequency shifting is implemented just like in the previous model. For simulation, the A part of the P1 symbol has the same FFT length as the data symbols and B part is the full copy of A part. Figure 6.10(a) presents the correlation and Figure 6.10(b) presents the MSE vs. SNR curve for timing synchronization.

The receiver processing chain has two frequency-shifter and running average filter combinations (Figure 5.7). Each frequency-shifter and running average filter will generate one correlation peak and a delay has been added to time align these two peak. The detection procedure is the same as the previous structures. If this correlation peak is present in the output of the receiver processing chain, then it can be concluded that the P1 symbol is present in that particular RF channel based on a carefully chosen threshold value.

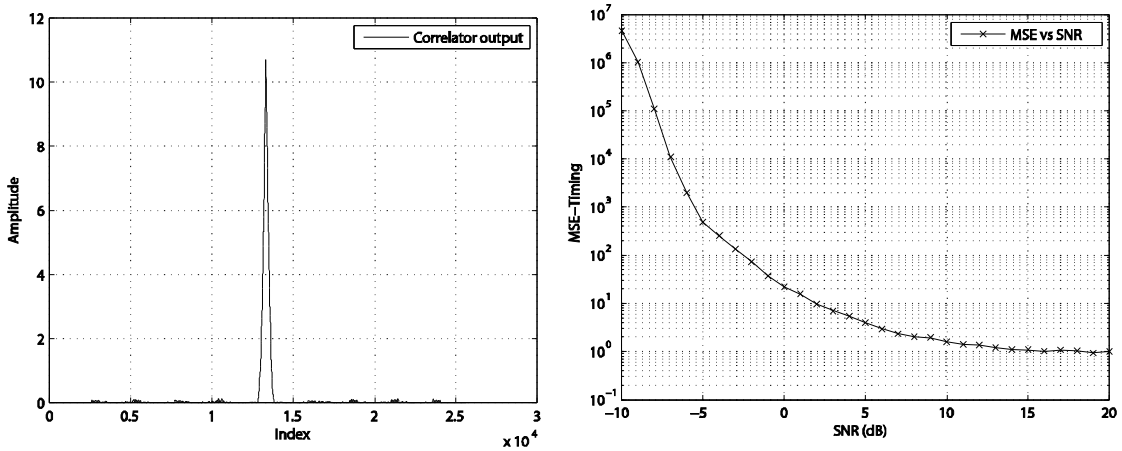

(a) (b)

Figure 6.10. *(a) Correlator output of receiver processing chain for C-A-B structure (b) MSE-Timing vs. SNR.*

The C-A-B structure is derived from the A-B shifted structure and therefore it can solve the problems of false detection, CW interferer and dangerous delays. The need for this C-A-B structure is to solve the problem of estimating the fractional part of the frequency offset from the argument of this correlator pulse. This was possible by A-B structure but was not possible by the A-B shifted structure. Figure 6.11 presents the MSE vs. SNR curve for estimating the fractional frequency offset for static Rayleigh channel and SFN channel. The amount of initial frequency offset introduced was 0.12. Therefore the C-A-B structure overcomes the problems of the previous structures.

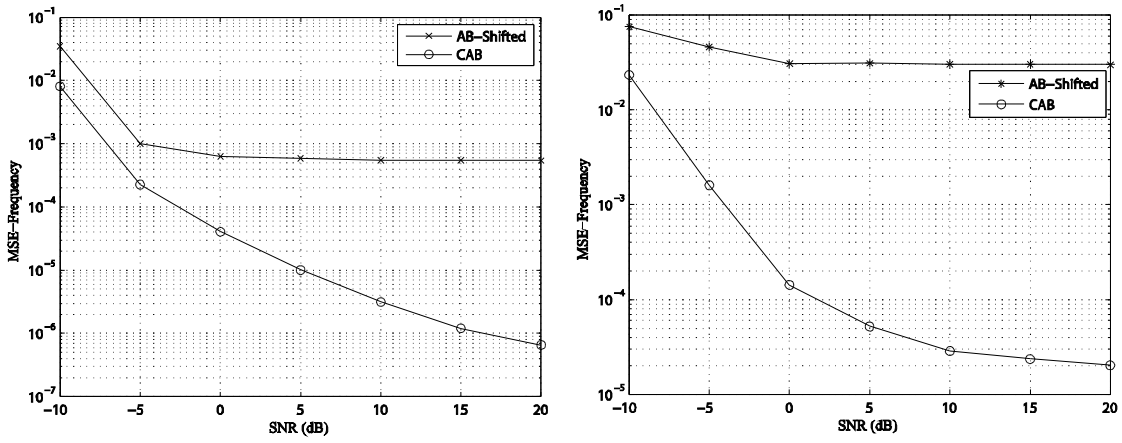

(a) (b)

Figure 6.11. *MSE-Frequency vs. SNR for constant frequency offset estimation (a) Rayleigh channel (b) SFN channel.*

6.3 Simulation model for P1 symbol

The simulation results in 6.2 shows that the final C-A-B structure for P1 symbol provides the better performance among other structures. Therefore, a slightly modified version of this C-A-B structure has been taken as the P1 symbol structure in the specification of DVB-T2 system. At the same time, the receiver processing chain was also modified. The simulation model for P1 Symbol has been created in Matlab according to the DVB-T2 standard [4] and DVB-T2 implementation guideline [19]. It considers two T2-frames, each starting with a P1 symbol and four data symbols. However, the observation window considers four data symbols of the first frame, and the P1 symbol and four data symbols of the second frame. The target of this simulation model is to simulate the reception process in the receiver in order to detect the presence of the P1 symbol, perform coarse timing synchronization task, and later decode the P1 symbol to know the basic transmission parameters.

In the transmitter, at first the data symbols are modulated in the frequency domain. Then these data symbols are transformed to time domain by Fast Fourier transformation. Then guard interval is added and normalization is done. P1 symbol is also generated in the frequency domain and later transformed into time domain signal. The process of P1 symbol generation is given in subsection 5.3.1.3 that elaborates the symbol structure, carrier distribution, modulation and time domain signal generation of the P1 symbol. Finally, the P1 symbol is placed in the beginning of the T2-frames. Therefore the transmitter emits a time domain signal that passes through the transmission channel and the receiver also receives the signal in time domain. A number of transmission channels are used to evaluate the performance of DVB-T2 systems. These channel models has been described in Chapter 4.

There are a number of important parameters that need to be set before proceeding to the next level. The OFDM data symbols in the T2-frames have two parts: the useful duration and the guard interval duration. DVB-T2 standard provides a number of choices for choosing the FFT-length representing the useful duration and guard interval duration of the data symbols. For simulation, 2k FFT-length has been chosen for the data symbol FFT-length and guard interval has been chosen as 1/4, meaning that 512 samples. In addition, four OFDM data symbols have been considered for the simulation in the two T2-frames of the observation window.

The simulation model in the receiver is modeled by the P1 symbol detection correlation chain discussed in subsection 5.3.1.4. If a P1 symbol is present in the RF channel, then this correlation chain will give a trapezoidal correlation pulse in the output. The presence of the P1 symbol, thus the DVB-T2 signal can be determined by setting a suitable threshold to the magnitude of the correlator output. The process of determining the threshold is crucial because the goal is to maximize the probability of detection and minimize the probability of false detection.

False detection refers to the fact that the receiver detects the presence of a P1 symbol when actually there is no P1 symbol present in the RF channel, meaning that, the receiver falsely gives a correlation output pulse above the threshold and concludes that a P1 symbol is present in the channel. So the threshold is chosen based on a compromise of these two factors. Moreover, the threshold is dependent on the number of data symbols chosen for the simulation. Therefore if the parameters of the simulation model are changed, for example, if the number of data symbols in the T2-frame is modified, then the appropriate threshold has to be calculated again.

However, the receiver has to identify the P1 symbol position in the received time domain signal in order to decode it. Here comes the case of achieving timing synchronization. One way to do that is to find the index of the correlation peak, and determine the start position from that index. However, the correlation peak for the receiver processing chain of P1 symbol produces a trapezoidal peak instead of a single triangular peak because of the P1 symbol structure that has two guard intervals in its both sides. Moreover, the highest peak value may be found within any duration of this trapezoidal shaped peak and therefore determining the starting position of the P1 symbol from this peak index is not consistent enough.

The alternative way that can be followed in the simulation model determines the starting position of the P1 symbol from the received signal and does not take the highest value of the peak into account. As mentioned previously, a threshold is used to detect the presence of the P1 symbol. That threshold will intersect the correlation output pulse at some point and the index of the first intersection point is calculated. It is assumed that the ideal P1 symbol position from the transmitted signal structure is known. If the index of the intersection point is subtracted from the ideal start position, then an offset value can be found.

This offset value added with the first intersection index will essentially give the starting index of the P1 symbol in the received signal. This offset value is first calculated at high SNR for AWGN channel in the mechanism discussed and later used in the simulation to determine the beginning of P1 symbol. The offset has to be estimated again if the parameters of the simulation model are changed, for example, if the number of data symbols in the simulation model is changed. Figure 6.12 elaborates the technique mentioned above showing the trapezoidal peak produced by the receiver processing chain.

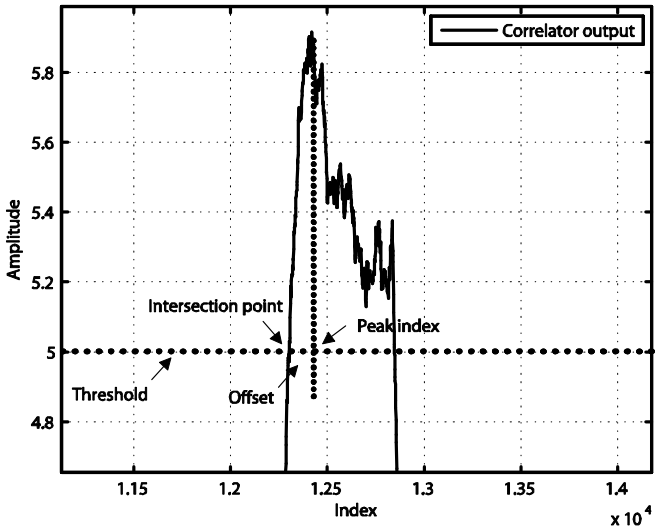

Figure 6.12. *Offset calculation for Trapezoidal correlation peak based on a threshold.*

After detecting the P1 symbol, the next step is to decode it in order to find the necessary transmission parameters. As discussed earlier, P1 symbol discloses the SISO/MISO parameter by its S2 field and FFT-length parameter by its S2 field. Therefore the simulation model has been developed such that these fields are encoded in the transmitter, then transmitted through the transmission channel and later decoded in the receiver. The performance is measured by the probability of decoding. If the transmitted data are decoded correctly, then the probability of decoding becomes higher. This is the desirable scenario because the reliability of the system depends on the probability of decoding.

Another important parameter is the SNR value in which the system is operating. For robust synchronization, DVB-T2 receiver has to be able to synchronize even at very low SNR around 0 dB. The remaining parameter for the simulation is the number of iterations of the simulation model in order to generate the appropriate performance measurement curves. A large number of iterations will provide a smooth

curve. On the other hand, a number of abrupt changes will be visible in curves if less number of iterations is used.

6.4 P1 symbol simulation performance

The first task of the DVB-T2 receiver is to detect the presence of P1 symbol in the channel. After detecting the P1 symbol, the receiver knows that DVB-T2 signal is present in the transmission channel. The next task is to determine the starting position of the P1 symbol, which is necessarily the starting position of the T2-frame. When the position of the P1 symbol is known to the receiver, then it can decode the P1 symbol in order to get the value of necessary transmission parameters. This subsection presents the related simulation results for P1 symbol detection and decoding.

Detection probability gives the probability of correctly detecting the P1 symbol in the transmission channel for a particular SNR value. On the other hand, decoding probability gives the probability of correctly decoding the P1 symbol for a particular SNR value. If it is possible to detect the P1 symbol, only then P1 symbol is decoded. It means that, when the P1 symbol is not detected, then the decoding probability is not calculated. In order to test the performance of P1 symbol, the detection and decoding probability are calculated for a range of SNR values for different channels, like AWGN channel, Ricean channel, Rayleigh channel, mobile TU6 channel and SFN channel, respectively. The common parameters used in all the simulations are given in Table 6.2.

Parameter	Value
FFT-length of the data symbols	2048
Guard Interval of the data symbols	512
Number of data symbols in each T2-frame	4
Signal-to-noise ratio (SNR)	-15 to 5 dB
Modulation in the data symbol	16-QAM
Modulation in the P1 symbol	DBPSK

Table 6.2: Parameters with their values for simulations.

The observation window for simulation considers two T2 frames such that at first it has the data frames of the first frame, then the P1 symbol of the second frame and at the end, the data symbols of the second frame. The observation window is given in Figure 6.13.

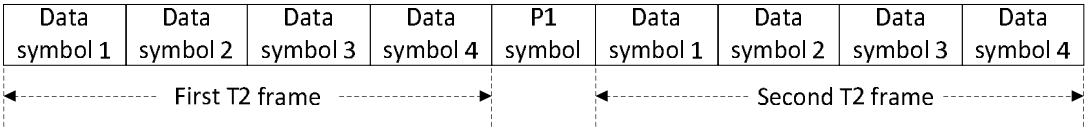

Figure 6.13. The observation window for simulation model.

As discussed in the previous section while describing about the simulation model for P1 symbol, an optimum threshold has to be chosen to calculate the detection probability. The target is to maximize the correct detection probability and at the same time, minimize the false detection probability. For calculating the false detection probability, a data symbol is sent instead of the P1 symbol and the probability of detecting that symbol is calculated. Figure 6.14 presents the correct detection and false detection probability for a varying range of threshold for AWGN channel.

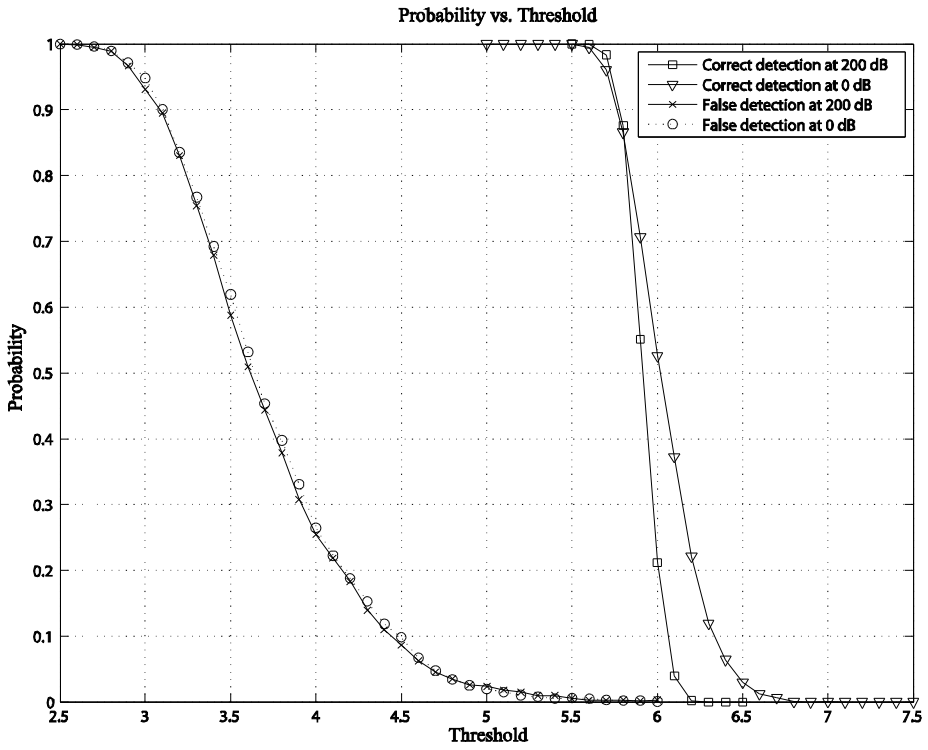

Figure 6.14. *Probability of correct and false detection vs. threshold.*

From Figure 6.14, it can be seen that the probability of correct detection goes to zero when the threshold is 6.2 for 200 dB. And for 0 dB, the detection probability goes to zero when the threshold is 6.8. On the other hand, the false detection probability for 200 dB and 0 dB, both reach zero when the threshold is near 5.5. A value from 5 to 5.5 can be chosen as the level of threshold because the false detection

probability is very low at this threshold value and at the same time, the detection probability is maximized. In this case, 5 has been chosen as the threshold value to be in the safe side because a steep for false detection probability can be observed just after threshold value of 5.5 in Figure 6.14.

The threshold value determined now is later used for simulation in other channels. However, this threshold is calculated for the particular transmission parameters given in Table 6.2. If they are modified, then that modification has to be taken into account and the optimum threshold value has to be determined again.

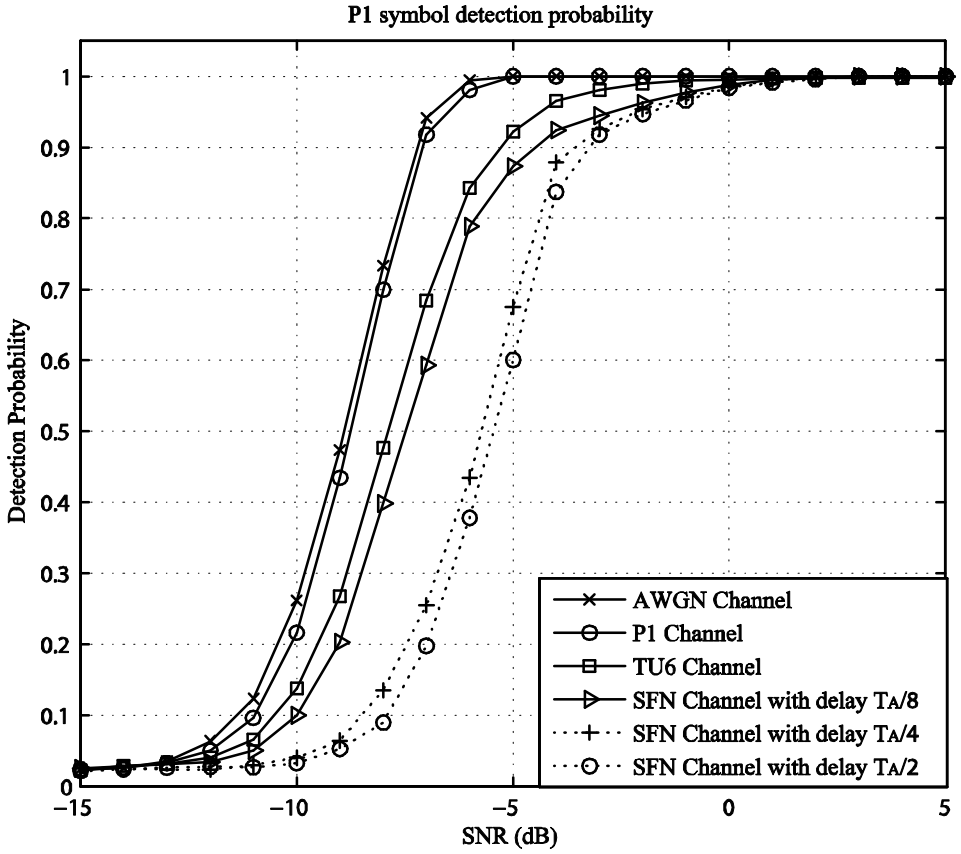

Figure 6.15. *P1 symbol Detection probability vs. SNR (dB) for threshold 5.*

After determining the appropriate threshold, the P1 symbol model has been simulated in order to calculate detection probability in AWGN, Rayleigh, mobile TU6 and SFN channels respectively for a range of SNR values. The result of simulation has been presented for all these channels in Figure 6.15. The TU6 channel has been modeled by two Rayleigh channels. The three SFN channels have been modeled having two Rayleigh paths having a delay of $T_A/8$, $T_A/4$, and $T_A/2$ between them, where T_A is the useful symbol duration of P1 symbol.

After detecting the P1 symbol, the offset is estimated in the receiver. The offset calculation has been described in the last subsection (Figure 6.12). Finally, this offset value is added with the intersection point to determine the exact starting position of the P1 symbol. This offset value is dependent on parameters chosen for simulation that are given in Table 6.2. Therefore if the settings of simulation are changed, then the offset has to be recalculated.

The calculated starting position of the P1 symbol is used for timing synchronization in the receiver. At this point, the receiver can decode the P1 symbol for determining the transmission parameters as it knows the appropriate starting position of the P1 symbol. The simulation result for decoding probability vs. SNR has been presented in Figure 6.16 for different channels. It can be seen that the decoding probability for SFN channel decreases when the delay between the paths of the SFN channel increases. It happens because of the presence of frequency selectivity in the SFN channel.

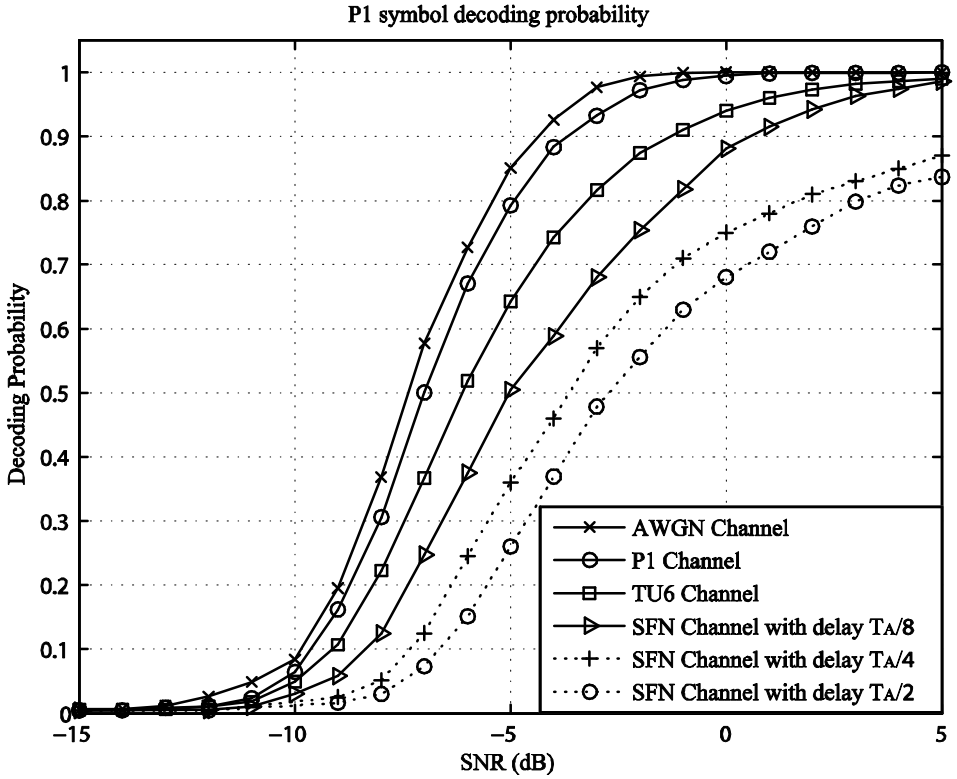

Figure 6.16. *P1 symbol Decoding probability vs. SNR (dB) for threshold 5.*

7. Conclusion

The synchronization of DVB-T2 system that can be achieved by P1 symbol is studied in this thesis. In other words, the purpose was to evaluate the performance of P1 symbol in different channels in order to achieve timing synchronization and frequency synchronization. It is important for the receiver to locate the received signal in both time and frequency by achieving synchronization before it can extract the transmitted information.

Synchronization in DVB-T2 system can be achieved by utilizing several features, for example, P1 symbol, P2 symbols, scattered pilots and continual pilots. The synchronization task can be divided into pre-FFT and post-FFT stages. Moreover, timing synchronization can be separated by coarse timing synchronization in pre-FFT stage and fine timing synchronization in post-FFT stage. Furthermore, fractional frequency synchronization can be achieved in pre-FFT stage and integer frequency synchronization can be achieved in post-FFT stage. This thesis focuses on the pre-FFT coarse timing synchronization and fractional frequency synchronization that can be achieved by P1 symbol.

The P1 symbol used in DVB-T2 identifies the presence of DVB-T2 signal in the transmission channel. It also marks the beginning of each T2 frame and each future-expansion-frame part and transmits basic transmission parameters like FFT size and SISO/MISO transmission mode. Most importantly, P1 symbol enables the receiver to accomplish synchronization before FFT by achieving coarse timing and fine frequency synchronization. Thus P1 symbol achieves some form of synchronization and saves time during the initial scanning and channel set up process.

The P1 symbol structure went through some evolution stages before being finalized in the DVB-T2 specification. The different structures of this evolution stages are presented with simulation results to describe the capabilities and drawbacks of each structure in order to show the need of the next structure. Simulation results show that the final C-A-B structure provides better performance for the P1 symbol structure. Hence, the actual P1 symbol structure in DVB-T2 system specification was inspired by the C-A-B structure and was finalized after making few modifications both in the symbol structure and in the corresponding receiver processing chain.

The simulation model for DVB-T2 system is implemented including the P1 symbol according to the implementation guideline for DVB-T2 system specification. For detecting the P1 symbol, a threshold has to be used in the correlation peak produced by the receiver processing chain. If the peak is above the threshold, then it is considered that the P1 symbol is detected. Therefore, determining this threshold is very important. However, one limitation of the simulation model is that the threshold has to be recalculated if the parameters of the simulation models are changed.

The output of the receiver processing chain produces a correlation peak which is not triangular. Instead, it is a trapezoidal peak. This single highest point in the trapezoidal peak changes from one iteration to another iteration. As a result, the highest peak calculation becomes difficult. Hence, the peak index has to be calculated in an alternative way.

Another limitation of the simulation model comes from this alternative method to calculate the peak index. The first intersection point of the threshold and the correlation peak is taken into account to calculate an offset that will lead to the peak index of the correlation. This offset has to be estimated again if the parameters of the simulation model are modified, for example, if the number of data symbols is changed.

This thesis concentrates on the synchronization in DVB-T2 system before FFT but the synchronization issues after FFT were left out. Synchronization after FFT includes fine timing synchronization and integer frequency offset determination. In order to achieve perfect synchronization, these methods have to be investigated. In the future, the research work will continue to evaluate the performance after achieving complete synchronization.

References

[1] DVB Project, http://www.dvb.org, referred July 5, 2009.

[2] ETSI EN 302 744 V. 1.6.1: Digital Video Broadcasting (DVB); Framing structure, channel coding and modulation for digital terrestrial television (DVB-T), Jan. 2009.

[3] ETSI EN 302 304 V. 1.3.1: Digital Video Broadcasting (DVB);,Transmission system for Handheld Terminals (DVB-H), Nov. 2004.

[4] ETSI EN 302 755 V. 1.1.1: Digital Video Broadcasting (DVB); Frame structure, channel coding and modulation for a second generation digital terrestrial television broadcasting system (DVB-T2), June 2008.

[5] J. Bingham, "Multicarrier Modulation for Data Transmission: An Idea Whose Time Has Come," in *IEEE Communications Magazine*, vol. 28 of 5, pp. 5-14, May 1990.

[6] R. Nee and R. Prasad, *OFDM Wireless Multimedia Communications.*: Artech House Boston London, 2000.

[7] J. Heiskala and J. Terry, *OFDM Wireless LANs: A Theoritical and Practical Guide*.: John Wiley and Sons Ltd, 2005.

[8] L. Litwin, "An Introduction to Multicarrier Modulation," in *IEEE Potentials*, vol. 19 of 2, pp. 36-38, May 2000.

[9] J. Rinne, "Performance and Analysis of OFDM for Digital TV Broadcasting Systems," Licentiate Thesis, Tampere University of Tecnology, 1994.

[10] S. Weinstein and P. Ebert, "Data Transmission by Frequency-Division Multiplexing Using the Discrete Fourier Transform," in *Communication Technology, IEEE Transactions*, vol. 1, pp. 628-634, 1971.

[11] G. Santella, R. Martino, and M. Ricchiuti, "Single Frequency Network (SFN) planning for digital terrestrial television and radio broadcast services: the Italian frequency plan for T-DAB," in *Vehicular Technology Conference, IEEE 59th*, vol. 4, pp. 2307-2311, 2004.

[12] J. C. Kim and J. Y. Kim, "Single Frequency Network Design of DVB-H (Digital Video Broadcasting - Handheld) System," in *Advanced Communication Technology*, vol. 3, pp. 1595-1598, 2006.

[13] J. Lee, H. Lou, D. Toumpakaris, and J. Cioffi, "Effect of Carrier Frequency Offset on OFDM Systems for Multipath Fading Channels," in *Global Telecommunications Conference, IEEE*, vol. 6, pp. 3721-3725, 2004.

[14] X. Ma, H. Kobayashi, and S. Schwarrz, "Effect of Frequency Offset on BER of OFDM and Single Carrier Systems," in *Personal, Indoor and Mobile Radio Communications*, vol. 3, pp. 2239-2243, 2003.

[15] C. Mushchallik, "Influence of RF Oscillators on an OFDM Signal," in *IEEE Transactions on Consumer Electronics*, vol. 41, pp. 592-603, August 1995.

[16] Q. Zou, A. Tarighat, and A. Sayed, "Compensation of Phase Noise in OFDM Wireless Systems," in *IEEE Transactions on Signal Processing*, vol. 55, pp. 5407-5424, 2007.

[17] S. Han and J. Lee, "An Overview of Peak-to-Average Power Ratio Reduction Techniques for Multicarrier Transmission," in *IEEE Wireless Communications*, vol. 12, pp. 56-65, 2005.

[18] DVB Document A114: Commercial Requirements for DVB-T2; April 2007. www.dvb.org.

[19] DVB Document A133: Implementation Guidelines for a Second Generation Digital Terrestrial Television Broadcasting System (DVB-T2), Feb. 2009, www.dvb.org.

[20] DVB-T2 Fact Sheet, Apr. 2009, www.dvb.org.

[21] S. Haykin and M. Moher, *Modern Wireless Communication*., Pearson Prentice Hall, 2005.

[22] B. Skalar, "Rayleigh Fading Channels in Mobile Digital Communication Systems Part I: Characterization," *IEEE Communications Magazine*, September, 1997.

[23] B. Bing, *Braodband Wireless Access*., Kluwer Academic Publishers, 2002.

[24] J. D. Parsons, *The Mobile Radio Propagation Channel*., Pentech Press Ltd, 1992.

[25] T. Ojanperä and R. Prasad, *Wideband CDMA for Third Generation Mobile Communications*.: Arctech House Publishers, 1997.

[26] S. Mathur, "Small Scale Fading in Radio Propagation," Department of Electrical Engineering, Rutgers University, Lecture notes for Wireless Communication Technologies course offered by Dr. N. Madhaban, Spring 2005.

[27] L. Cheng, B. Henty, F. Bai, and D. D. Stancil, "Doppler Spread and Coherence Time of Rural and Highway Vehicle-to-Vehicle Channels at 5.9 GHz," in *Global Telecommunications Conference*, pp. 1-6, 2008.

[28] R. N. Pupala, "Introduction to Wireless Electromagnetic Channels & Large Scale Fading," Department of Electrical Engineering, Rutgers University, Lecture notes for Wireless Communication Technologies course offered by Dr. N. Madhaban, Spring 2005.

[29] T. S. Rappaport, *Wireless Communications: Principles and Practice*., Prentice Hall, 2002.

[30] M. Simon and M. Alouini, *Digital Communication Over Fading Channels*., 2nd Edition, John Wiley & Sons, Inc., 2005.

[31] "COST 207: Digital Land Mobile Radio Communications (Final report)," Commission of the European Communities, Directorate General Telecommunications, Information Industries and Innovation, pp. 135-147, 1989.

[32] A. Gallardo, M. Woodward, and J. Rodriguez-Tellez, "Performance of DVB-T

OFDM based Single Frequency Networks: Effects of Frame Synchronisation, Carrier Frequency Offset and Non-Synchronised Sampling Errors," in *Vehicular Technology Conference*, vol. 2, pp. 962-966, 2001.

[33] A. Mattsson, "Single Frequency Networks in DTV," in *IEEE Transactions on Braodcasting*, vol. 51, Deceember 2005.

[34] B. Ai, Z. Yang, C. Pan, J. Ge, and Y. Wang, "On the Synchronization Techniques for Wireless OFDM Systems," in *IEEE Transactions on Broadcasting*, vol. 52, no. 2, June 2006.

[35] A. Palin and J. Rinne, "Symbol Synchronization in OFDM System for Time selective Channel conditions," in *IEEE International Conferenec on Electronics, Circuits and Systems*, vol. 3, pp. 1581-1584, September 1999.

[36] J. J. van de Beek, M. Sandell, and P. O. Börjesson, "ML Estimation of Time and Frequency Offset in OFDM Systems," in *IEEE Transactions on Signal Processing*, vol. 45, no. 7, July 1997.

[37] D. Liu and J. Chung, "Enhanced OFDM Time and Frequency Synchronization Through Optimal Code Correlation," in *Circuits and Systems*, vol. 1, pp. 176-179, August 2002.

[38] S. A. Fetchel, "OFDM Carrier and Sampling Frequency Synchronization and Its Performance on Stationary and Mobile Channels," in *IEEE Transactions on Consumer Electronics*, vol. 46, no. 3, August 2000.

[39] B. Jahan, M. Lanoiselée, G. Degoulet, and R. Rabineau, "Full Synchronization Method for OFDM/OQAM and OFDM/QAM Modulations," in *Spread Spectrum Techniques and Applications*, pp. 344-348, Aug 2008.

[40] J. Stott, "The P1 symbol," BBC research, Presentation given in DTG DVB-T2 Implementers' Seminar, London, 9th Octobor, 2008.

[41] X. Wang, Y. Wu, J. Chouinard, S. Lu, and B. Caron, "A Channel Characterization Technique Using Frequency Domain Pilot Time Domain Correlation Method for DVB-T Systems," in *IEEE Transaction on Consumer Electronics*, vol. 49, no. 4, pp. 949-957, November 2003.

[42] A. Filippi and S. Serbetli, "OFDM Symbol Synchronization Using Frequency Domain Pilots in Time Domain," in *Proceedings of Vehicular Technology Conference*, pp. 1376-1380, October 2007.